

Causal exposure-response curve estimation with surrogate confounders: a study of air pollution and children’s health in Medicaid claims data

Jenny J. Lee¹, Xiao Wu², Francesca Dominici¹, and Rachel C. Nethery¹

¹Department of Biostatistics, Harvard T.H. Chan School of Public Health, Boston, MA

²Department of Biostatistics, Mailman School of Public Health, Columbia University, New York, NY

Abstract

In this paper, we undertake a case study in which interest lies in estimating a causal exposure-response function (ERF) for long-term exposure to fine particulate matter (PM_{2.5}) and respiratory hospitalizations in socioeconomically disadvantaged children using nationwide Medicaid claims data. New methods are needed to address the specific challenges the Medicaid data present. First, Medicaid eligibility criteria, which are largely based on family income for children, differ by state, creating socioeconomically distinct populations and leading to clustered data, where zip codes (our units of analysis) are nested within states. Second, Medicaid enrollees’ individual-level socioeconomic status, which is known to be a confounder and an effect modifier of the exposure-response relationships under study, is not available. However, two useful surrogates are available: median household income of each enrollee’s zip code of residence and state-level Medicaid family income eligibility thresholds for children. In this paper, we introduce a customized approach, called *MedMatch*, that builds on generalized propensity score matching methods for estimating causal ERFs, adapting these approaches to leverage our two surrogate variables to account for potential confounding and/or effect modification by socioeconomic status. We conduct extensive simulation studies, consistently demonstrating the strong performance of *MedMatch* relative to conventional approaches to handling the surrogate variables. We apply *MedMatch* to estimate the causal ERF between long-term PM_{2.5} exposure and first respiratory hospitalization among children in Medicaid from 2000 to 2012. We find a positive association, with a steeper curve at PM_{2.5} $\leq 8 \mu\text{g}/\text{m}^3$ that levels off at higher concentrations.

Keywords: Generalized propensity score; Matching; Fine particulate matter; Socioeconomic status; Medicaid eligibility thresholds.

1 Introduction

In the United States, the Clean Air Act explicitly requires the primary national ambient air quality standards to be sufficient to protect the health of sensitive populations, such as socioeconomically disadvantaged children. Children are known to be more susceptible to air pollution exposure as it can disrupt their respiratory, neurological, and immune systems, which are still developing and immature. It is relatively well known that exposure to ambient air pollution, and in particular to fine particulate matter ($PM_{2.5}$), has adverse health effects on children (World Health Organization, 2018). However, there has been minimal characterization of the adverse effects of long-term $PM_{2.5}$ exposure on socioeconomically disadvantaged children, who may be more vulnerable to its effects due to increased exposure, increased prevalence of underlying diseases, or inadequate resources to implement precautionary measures (Cortes-Ramirez et al., 2021).

In this paper, we seek to study the effect of long-term $PM_{2.5}$ exposure on respiratory hospitalization in low-income children using claims data from the US Medicaid program for the period 2000-2012. Medicaid insures nearly 40% of US children, who must come from a low-income family or be disabled in order to qualify (Truffer et al., 2016). The Medicaid program is jointly funded by the state and federal governments. However, the program is administered by the states, and each state can determine how low a family’s income must be in order for the children to be Medicaid eligible (the “eligibility threshold”) (Figure 1). Therefore states with vastly differing Medicaid eligibility thresholds will have socioeconomically distinct Medicaid populations. As a result of the state-level heterogeneity in Medicaid program administration and characteristics of enrollees, Medicaid claims data can be viewed as having a clustered structure where units (either individuals or small areas, such as zip codes) are nested within states. In our motivating application, we assume that zip codes are the units of analysis, and they are clustered within state.

Income is known to be associated with both $PM_{2.5}$ and respiratory outcomes, i.e., it is a confounder of the association of interest (Greenland et al., 1999; Hajat et al., 2021). In addition, the causal effect of $PM_{2.5}$ varies in the direction and/or magnitude by income levels, i.e., income is an effect modifier (VanderWeele and Robins, 2007; Cakmak et al., 2016; Hajat et al., 2021). Even in Medicaid-enrolled children, a population that is generally low-income, substantial variability in income remains; thus, it is likely to exert a confounding and effect modifying influence. However, Medicaid claims data do not provide individual-level information on the income of the beneficiaries (when using data for children, we would like to know each child’s *household income*). However, we

Medicaid Eligibility Thresholds in 2005 (Age 6-18)

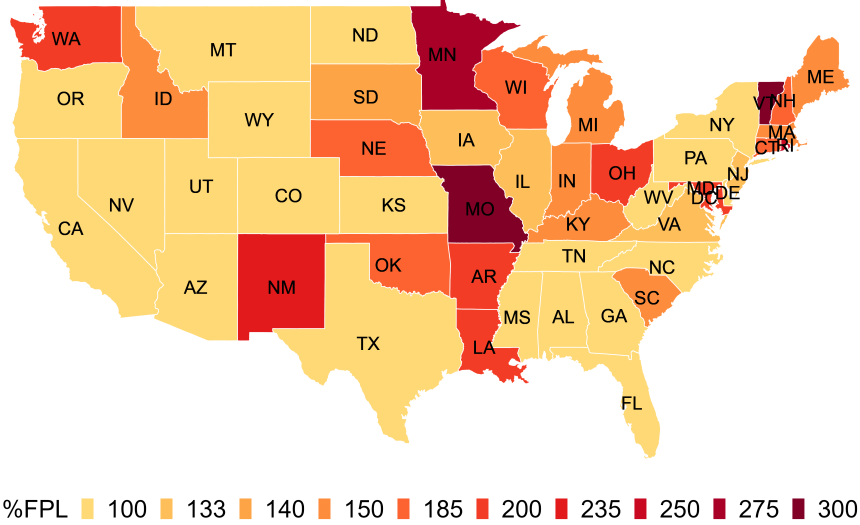


Figure 1: US map of each state’s Medicaid family income eligibility thresholds for children of age 6-18, calculated as a percentage of the federal poverty level (%FPL) in 2005. The darker red indicates higher %FPL, i.e., a less stringent eligibility threshold. There were 10 distinct Medicaid eligibility thresholds used by states in 2005.

have available two useful surrogates: 1) the median household income of the zip code of residence of each Medicaid enrollee (note that this is the median across the entire zip code population, not restricted to Medicaid enrollees in the zip code); and 2) the state-level Medicaid family income eligibility thresholds for children, calculated as a percentage of the federal poverty level (Brooks et al., 2019).

In this paper, we propose a causal inference method in the context of clustered data with surrogate measures called *MedMatch*. *MedMatch* is a customized approach that can estimate a causal exposure-response function (ERF) for $PM_{2.5}$ in Medicaid claims data, accounting for the potential confounding and effect modifying influence of income for Medicaid-enrolled children using the two surrogate measures described above.

We posit two critical assumptions about the structure of the relationship between the unmeasured income variable and the surrogate variables, which will be leveraged by *MedMatch*. To better contextualize these assumptions, first recall that zip codes serve as units of analysis here, so in practice, we conceive of all confounders/effect modifiers in their zip code-aggregate version. Thus, the ideal income measure (which is unobserved in our data) is the median household income for Medicaid-enrolled children (MHI-MC) within each zip code. Then, our first assumption is that a state’s eligibility threshold is an upper bound of the MHI-MC of each of its zip codes. This

assumption follows directly from the stated policy that only individuals with income less than their state’s threshold are eligible to enroll, thus the MHI-MC must also be less than the threshold. Second, we assume that the zip code median household income (for all residents of the zip code) is a rank-preserving function of the zip code MHI-MC *within a state or across states with similar eligibility thresholds*. For example, within State A, if zip code A_1 has a higher median household income than zip code A_2 , zip code A_1 should also have higher MHI-MC than zip code A_2 (Figure 2). However, for two zip codes located in states with different eligibility thresholds, we do not make this rank-preserving assumption (Figure 2). For example, consider a zip code B_1 from state B and zip code A_1 from state A, where state B has higher eligibility threshold than state A. Even if the median household income in B_1 and A_1 are the same, we expect that the MHI-MC in B_1 will be larger because higher-income children in zip code B_1 will be Medicaid eligible thanks to the higher eligibility threshold.

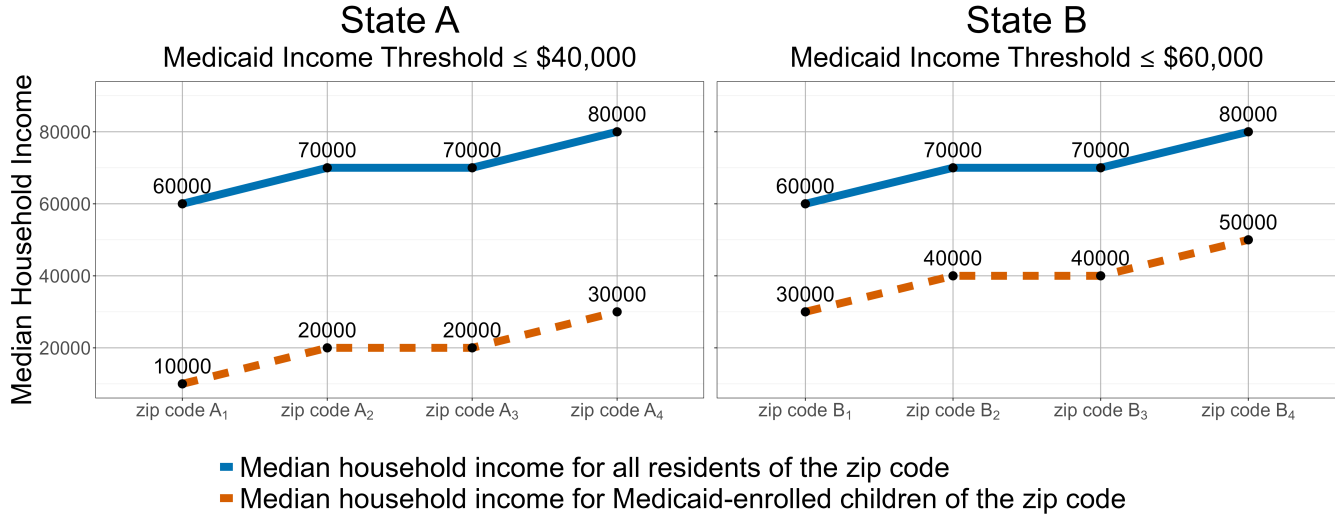


Figure 2: A toy example of the assumed relationship between median household income of the entire zip code and median household income of Medicaid-enrolled children in the zip code, for two states with different Medicaid eligibility thresholds.

These assumptions imply that, within a state or a set of states with the same eligibility threshold, we could proceed with usual procedures for causal inference to estimate the effect of $PM_{2.5}$ on respiratory hospitalizations, using zip code median household income directly as a surrogate for MHI-MC. In the context of clustered data, causal matching methods have been proposed that require or encourage within-cluster matching (Thoemmes and West, 2011; Rickles and Seltzer, 2014; Arpino and Cannas, 2016; Kim and Steiner, 2015). However, the above approaches may be

insufficient in our setting for several reasons. First, when cluster sizes are small, strict within-cluster matching may perform poorly due to the difficulty of finding appropriate matches and balancing covariates within clusters. Second, the methods that encourage within-cluster matching require subjective user-specification of critical parameters quantifying how poor the within-cluster matching options must be to warrant searching for matches across clusters. Third, all of the above methods require a binary treatment/exposure variable.

In the context of air pollution epidemiology, preserving the inherent continuity of exposures is critical. However, only a few recent papers have begun to propose causal inference methods for estimating an ERF with continuous treatments/exposures, exclusively designed for single-level data. Existing approaches include the adjustment for the estimated generalized propensity score (GPS) in the outcome model (Hirano and Imbens, 2004); a doubly robust kernel smoothing approach (Kennedy et al., 2017); GPS matching (Wu et al., 2022); and Gaussian processes (Ren et al., 2021).

Our proposed *MedMatch* method builds on the GPS matching approach of Wu et al. (2022), adapting it to account for the confounding and/or effect modifying influence of unmeasured MHI-MC in our analysis by carefully utilizing the surrogates and their assumed relationships with MHI-MC, while also balancing bias and variance. *MedMatch* has the following two key features: (1) it uses zip code median household income to construct the GPS and (2) it introduces a two-part matching target that seeks matches with comparable GPS values while also promoting matches within a state or across states with similar eligibility thresholds. We evaluate the performance of *MedMatch* via an extensive simulation study, and we apply it to estimate a causal ERF for long-term $PM_{2.5}$ exposure and respiratory hospitalization in children using nationwide Medicaid data.

The rest of the paper is constructed as follows. In Section 2, we introduce notation, the estimands of interest, and causal identifying assumptions, then we describe the proposed method. In Section 3, we conduct simulation studies and show that our proposed methods outperform several competitor methods. In Section 4, we present the results of the real data analysis. In Section 5, we summarize our findings, discuss the strengths and limitations of our method, and propose possible extensions.

2 Methods

2.1 Notation and estimand

The notation below follows Wu et al. (2022). Let $j = 1, \dots, N$ index the units of analysis (zip codes in our motivating data). Suppose W_j denotes the observed continuous exposure for unit j , and $\mathbf{C}_j = (C_{1j}, \dots, C_{pj}) \in \mathbb{R}^p$ denotes a vector of p measured covariates. Let Z_j be a special continuous covariate that has to be measured in traditional GPS matching approaches, but in our proposed method, we will allow it to remain unmeasured while utilizing measured surrogates as substitutes. Two surrogate variables are measured - a continuous unit-level surrogate of Z (Z^*) and an integer-valued cluster-level variable (U) that leads to heterogeneity in the distribution of Z . In our motivating Medicaid data, Z is the unmeasured zip code-level MHI-MC, Z^* is the measured median household income of the total zip code population, and U is the Medicaid eligibility threshold of the state containing each of the zip codes, which is common across all zip codes within a state (i.e., it is a cluster-level variable). Y_j is the observed outcome, assumed here to be continuous. Under the standard Stable Unit Treatment Value Assumption (SUTVA) for causal inference, we define $Y_j(w)$ to be the counterfactual outcome for unit j at exposure level w (Rubin, 1974, 1980). Let $f(w | \mathbf{c}, z)$ be the true GPS, i.e., the conditional probability density function of exposure level w given covariates \mathbf{c} and z . We aim to estimate the population average causal ERF $\mu(w) = E[Y(w)]$ for exposures $w \in \mathbb{W}$, where the expectation is taken over the distribution of counterfactual outcomes in the population of interest.

2.2 Causal ERF identifying assumptions and within-cluster matching

We first present assumptions that are sufficient to allow the causal ERF to be identified under the surrogate variable framework described above. Recall the structure of the relationships between these variables posited in Section 1: Z^* is a rank-preserving function of Z within levels of U . In this setting, the standard identifying assumptions for causal ERFs given by Wu et al. (2022), must be adapted so that unconfoundedness can be obtained when relying on Z^* and U rather than Z .

Assumption 1 (Consistency). *If $W_j = w$, then $Y_j = Y_j(w)$.*

Assumption 1 states that each unit’s observed outcome is equal to its potential outcome at its observed exposure level.

Assumption 2 (Overlap). $f(w | \mathbf{c}, z) > 0$ for any \mathbf{c} , z , and exposure level $w \in \mathbb{W}$.

Assumption 2, known as the overlap or positivity assumption, states that each unit in the dataset should have positive probability of receiving each exposure level.

Assumption 3 (Local Weak Unconfoundedness). $I(W_j = \tilde{w}) \perp\!\!\!\perp Y_j(w) | \mathbf{C}_j, Z_j$, for any $w \in \mathbb{W}$ and \tilde{w} is in a neighborhood set around w (i.e., $\tilde{w} \in [w - \delta, w + \delta]$).

Assumption 3 states that conditioning on C and Z is sufficient to eliminate confounding. Wu et al. (2022) show that, under the local weak unconfoundedness assumption, unconfoundedness also holds when conditioning on the GPS rather than the full vector of covariates, i.e., $I(W_j = \tilde{w}) \perp\!\!\!\perp Y_j(w) | f(\tilde{w} | \mathbf{C}_j, Z_j)$.

Assumption 4 (Smoothness). Define $\mu_{\text{GPS}}(w, f) \equiv E[Y_j(w) | f(W_j | \mathbf{C}_j, Z_j), W_j = w]$ for any $w \in \mathbb{W}$. Then, for any $w, w' \in \mathbb{W}$, $|f(w | \mathbf{c}, z) - f(w' | \mathbf{c}, z)| \leq A |w - w'|$ and $|\mu_{\text{GPS}}(w, f) - \mu_{\text{GPS}}(w', f)| \leq B |w - w'|$ for some constant A and B .

Assumption 4 states that the continuity of the ERF is maintained over the exposure interval.

Assumption 5 (GPS with surrogates). Define the surrogate GPS, $f(w|c, z^*)$, as the density of W conditional on confounders C and surrogate confounder Z^* and let $d(\cdot, \cdot)$ be the total variation distance between two probability distributions. Then, $d(f(w|C_j, Z_j), f(w|C_k, Z_k)) = d(f(w|C_j, Z_j^*), f(w|C_k, Z_k^*))$ when $U_j = U_k = u$.

Assumption 5 states that the distance between the conditional density functions for two units j and k with the same value of U is the same regardless of whether conditioning on Z or Z^* . This implies that, within levels of U , we can condition on the surrogate GPS rather than the true GPS to achieve unconfoundedness, i.e.,

$$I(W_j = \tilde{w}) \perp\!\!\!\perp Y_j(w) | f(\tilde{w}; \mathbf{C}_j, Z_j^*), U. \quad (1)$$

We discuss how this assumption can be operationalized later in the section. Hereafter, to avoid confusion with the true GPS, we use the notation $e(w; \mathbf{c}, z^*) = f(w|c, z^*)$ for the surrogate GPS.

Under Assumptions 1-5, the population average causal ERF $\mu(w) = E[Y_j(w)]$ is identifiable, as it can be represented as the average over conditional expectations of observed outcomes conditioning

on $f(W_j; \mathbf{C}_j, Z_j^*)$, U , and exposure $W_j \in [w - \delta, w + \delta]$. Formally,

$$\mu(w) = E[Y_j(w)] = \lim_{\delta \rightarrow 0} E[E\{Y_j^{obs} \mid e(W_j; \mathbf{C}_j, Z_j^*), U, W_j \in [w - \delta, w + \delta]\}].$$

Under these identifying assumptions, strict within-cluster matching on the surrogate GPS would, in principle, avoid introducing any bias due to the unmeasured Z . Specifically, we could apply a fully stratified matching approach in which we (1) conduct GPS estimation and matching as in Wu et al. (2022) separately within levels of U , substituting Z^* for Z , then (2) combine the matched datasets across the clusters and proceed with ERF estimation. Hereafter, we refer to this as the *Within* matching approach. We describe in more detail the recommended procedures for *Within* matching below, and we discuss its limitations under small-to-moderate sample sizes.

The form of the GPS and surrogate GPS are generally unknown in real data, and thus we must estimate the surrogate GPS. Throughout this paper, following Wu et al. (2022), we assume a Normal conditional density for the GPS and surrogate GPS. Recall that Assumption 5 requires that, for two units with the same observed U values, the distance between the GPS densities for the two units and the distance between the surrogate GPS densities for the two units must be equal. In an effort to operationalize Assumption 5, we propose estimating the surrogate GPS for *Within* matching as follows. The conditional means are estimated using tree-ensemble models with C and Z^* as predictors, stratified on U (the use of tree-based models is key to operationalizing Assumption 5, as explained below). The variance is assumed to be constant and is estimated via the sample variance of the tree ensemble residuals. The surrogate GPS values are then estimated by plugging in estimates of the conditional means and variance into a Normal density function. Tree-based models, used to estimate the conditional means, are built using a sequence of binary splits on covariates, where the split points are selected to minimize a specified loss function computed from the outcomes in the partitions created by the split; thus, they are invariant to rank-preserving transformations of covariates. Per our assumptions, Z^* is a rank-preserving function of Z within levels of U ; hence, the fits of tree-ensembles within levels of U should be equivalent whether using Z or Z^* . If Z were observed, under this estimation strategy the estimated GPS (plugging in Z) and estimated surrogate GPS (plugging in Z^*) should be exactly equal. Thus, this would empirically satisfy Assumption 5.

Once the surrogate GPS have been estimated, *Within* matching can identify matches for each unit exactly following the procedures outlined in Wu et al. (2022), executed within each level of U

separately. We briefly describe these procedures here. At a high level, the objective of standard GPS matching is to eliminate confounding by creating a matched pseudo-population in which the distributions of observed confounders are balanced across exposure levels. To achieve this, GPS matching does the following: for any given exposure level $w^{(l)}$ and unit j , find a matched unit k that is its nearest neighbor in terms of a matching target function measuring 1) the distance between $w^{(l)}$ and w_k , to ensure that the selected match k has observed exposure level close to $w^{(l)}$ and 2) the distance between the estimated GPS of the two units at/near pseudo-exposure level $w^{(l)}$, i.e., it prioritizes find a matched unit k that had similar probability of receiving exposure $w^{(l)}$ to that of unit j , based on observed covariates. It repeats this procedure, selecting matches with replacement for each unit and each exposure level, to obtain a matched dataset. In *Within* matching, this can, in principle, be done separately for each level of U using the surrogate GPS, and the matched datasets from all the clusters combined. A smooth ERF can then be estimated by fitting a kernel smoother to the full matched dataset.

The *Within* matching approach most directly operationalizes the identifying assumptions, i.e., the surrogate GPS values are estimated using a strategy compatible with Assumption 5, and surrogate GPS matches are sought only within cluster under the assumption that the surrogate GPS is valid for confounding adjustment only within clusters (equation 1). Thus, *Within* matching should, in principle, eliminate bias due to measured confounders. However, empirical assessments have found that GPS matching methods for continuous exposures perform poorly under small-to-moderate sample sizes (Cork et al., 2023). In our real data, some levels of U consist of a relatively small number of units, with minimum 825 units (Figure S7). This means that finding adequate matches for all units at all exposure levels within their own clusters is likely to be impossible, and GPS match quality has to be sacrificed to enforce matching within clusters, which could induce residual confounding by the covariates summarized in the surrogate GPS. In short, when conducting *Within* matching in a setting with small-to-moderate sized clusters, the flexibility of GPS matching combined with small sample sizes lead to high-bias and high-variance estimates (Cork et al., 2023). Moreover, *Within* matching is unappealing in many scenarios because it requires manually tuning surrogate GPS models and matching procedures within each cluster.

2.3 Proposed *MedMatch* Method

In this section, we describe our proposed alternative matching approach, called *MedMatch*, for the estimation of a population average causal ERF while overcoming the challenges of small-to-moderate cluster sample sizes, as explained above. *MedMatch* utilizes analogous procedures to the standard GPS matching algorithm but utilizes the surrogate GPS and defines an alternative matching target function. In practice, *MedMatch* allows a limited amount of shared information across levels of U to achieve low bias and low variance simultaneously. First, *MedMatch* estimates the surrogate GPS values using tree ensemble models fit to the full data, not stratified on U . Second, it encourages, but does not force, matching within levels of U . Namely, for a given unit for whom a match is sought, the matching target of *MedMatch* finds matches with comparable surrogate GPS values while promoting matches within a cluster or across clusters with similar U values.

The detailed *MedMatch* procedures are as follows: We first define L equally sized exposure windows based on a pre-defined caliper of δ , where the caliper is defined as the diameter of the neighborhood set for any exposure level w , i.e., $[\min(w), \min(w) + \delta]$, $[\min(w) + \delta, \min(w) + 2\delta]$, \dots , $[\min(w) + (L - 1)\delta, \min(w) + L\delta]$ where $\min(w) = \min_{\{j \in \{1, \dots, N\}\}} w_j$. We define the mid points of the exposure windows as “pseudo-exposure” values, $w^{(l)} = \min(w) + \frac{2l-1}{2}\delta$ for $l = 1, \dots, L$. We then seek to approximate the counterfactual outcome for each unit at each pseudo-exposure level $w^{(l)}$ by finding a matched unit that experienced exposure within a window of size δ centered at $w^{(l)}$.

At each pseudo-exposure level $w^{(l)}$, our matching function selects a matched unit $j(w^{(l)})$ for each unit $j = 1, \dots, N$ based on two criteria: 1) to ensure the matched unit has observed exposure near $w^{(l)}$, its observed exposure $w_{j(w^{(l)})}$ must lie within δ caliper of $w^{(l)}$ (i.e., $w_{j(w^{(l)})} \in [w^{(l)} - \frac{1}{2}\delta, w^{(l)} + \frac{1}{2}\delta]$) and 2) to ensure two units are comparable in terms of both estimated surrogate GPS and U , the matched unit must be the nearest neighbor of the observed unit j (among the subset of units meeting criterion 1) based on a two-dimensional distance calculated using the estimated surrogate GPS and U , on a standardized scale. Specifically, we define the *MedMatch* matching function as follows:

$$j(w^{(l)}) = \arg \min_{j': |w_{j'} - w^{(l)}| \leq \delta} \left\{ \tau \left\| (\hat{e}_j^*(w^{(l)}, \mathbf{c}_j, z_j^*), \hat{e}_{j'}^*(w_{j'}, \mathbf{c}_{j'}, z_{j'}^*)) \right\| + (1 - \tau) \left\| (U_j^*, U_{j'}^*) \right\| \right\}. \quad (2)$$

where $\|\cdot\|$ is the distance metric (e.g. L_1 or L_2 distance), $\hat{e}_j^*(w^{(l)}, \mathbf{c}_j, z_j^*)$ and $\hat{e}_{j'}^*(w_{j'}^*, \mathbf{c}_{j'}, z_{j'}^*)$ are the

standardized estimated surrogate GPS values (standardization procedure described below) based on the fitted surrogate GPS model on the observed data at the pseudo exposure $w^{(l)}$ for unit j and at the observed exposure $w_{j'}$ for unit j' , respectively. $\tau \in [0, 1]$ is a scale parameter that weights between the estimated surrogate GPS and U , with very high values of τ favoring selection of matches with surrogate GPS very close to that of unit j , regardless of cluster, and low τ favoring matches within cluster. e^* and w^* represent the standardized versions of e and w to put the two measures on a comparable scale, i.e., $w^* = \frac{w - \min(w)}{\max(w) - \min(w)}$ and $e^* = \frac{e - \min(\hat{e})}{\max(\hat{e}) - \min(\hat{e})}$. We allow matching with replacement: a single unit can serve as a match for multiple other units. Then, the missing potential outcome of j at pseudo-exposure level $w^{(l)}$ is imputed using the observed outcome of the matched unit $j(w^{(l)})$, i.e., $\hat{Y}_j(w^{(l)}) = Y_{j(w^{(l)})}^{obs}$.

To assess whether the observed covariates are balanced across all exposure levels after the matching, the absolute correlation (AC) between exposure and each of the covariates are calculated in the matched dataset (Wu et al., 2022). Formally, suppose the j -th unit with exposure w_j and a covariate c_{1j} appears k_j times in the matched dataset. We calculate AC for a covariate Z in the matched dataset as

$$\rho_Z = \left| \sum_{j=1}^N k_j (\Sigma_{c_1}^{-1/2} (c_{1j} - \bar{c}_1)) (\Sigma_w^{-1/2} (w_j - \bar{w})) \right|$$

where $\bar{\cdot}$ denotes a weighted mean (i.e., $\bar{c}_1 = \sum_{j=1}^N k_j c_{1j} / \sum_{j=1}^N k_j$ and $\bar{w} = \sum_{j=1}^N k_j w_j / \sum_{j=1}^N k_j$) and Σ_{\cdot} denotes a weighted sampled variance (i.e., $\Sigma_{c_1} = \sum_{j=1}^N k_j (c_{1j} - \bar{c}_1)(c_{1j} - \bar{c}_1)^T / \sum_{j=1}^N k_j$, $\Sigma_w = \sum_{j=1}^N k_j (w_j - \bar{w})(w_j - \bar{w})^T / \sum_{j=1}^N k_j$) in the matched data. If covariate balance is achieved, the AC between the exposure and each covariate should be either equal to zero or close to it. Because the primary aim of matching is to balance the observed covariates, we select hyperparameters (δ, τ) that minimize the average of ACs across controlled covariates $\{\mathbf{C}, Z^*, U\}$ using a grid search approach. We set the threshold for achieving covariate balance to be average of ACs less than 0.1 (Zhu et al., 2015).

After implementing matching, a smoothed average ERF $\hat{\mu}(w) = \hat{\mathbb{E}}[Y(w)]$ across the range of exposures $w \in [\min(w), \max(w)]$ is obtained by fitting a kernel smoother on the entire matched dataset where an optimal bandwidth was chosen to minimize the risk function described in Kennedy et al. (2017).

2.4 Uncertainty estimation

We use m-out-of-n bootstrap to construct a point-wise Wald confidence band for the causal ERF as proposed by Wu et al. (2022). In brief, to create a bootstrap dataset $b = 1, \dots, B$, we resample m units out of N total units in the original dataset ($m < N$) with replacement. To preserve the clustered structure of the data, we resample a fixed number of units from each cluster to ensure that each cluster is represented proportionally to its representation in the original data. In each re-sampling, we re-calculate the GPS to account for variability in the model estimates. Then, we implement the proposed method on each bootstrap dataset, b , and obtain point-wise bootstrap estimates $\hat{\mu}_b(w)$, $b = 1, \dots, B$. Based on the bootstrap point estimates, we calculate the bootstrap variance as $\widehat{\text{Var}}[\hat{\mu}(w)] = \frac{m}{N} \frac{1}{B} \sum_{b=1}^B [\hat{\mu}_b(w) - \frac{1}{B} \sum_{r=1}^B \hat{\mu}_r(w)]^2$. Note that the correction term $\frac{m}{N}$ is included to account for the difference in sample size between the bootstrap and the original dataset. Then, we build a Wald $100(1 - \alpha)\%$ confidence interval as $\hat{\mu}(w) \pm z_{1-\frac{\alpha}{2}} \times \sqrt{\widehat{\text{Var}}[\hat{\mu}(w)]}$, where $z_{1-\alpha/2}$ denotes the $(1 - \frac{\alpha}{2})$ quantile of a standard normal distribution.

3 Simulations

3.1 Simulation settings

The data generating mechanism for the simulation studies is informed by those in Kennedy et al. (2017) and Wu et al. (2022). We generate $N = 2,000$ samples falling into G distinct clusters. We generate five measured covariates $\mathbf{C} = (C_1, \dots, C_5)$ as follows: $(C_1, C_2, C_3) \sim MVN(\mathbf{0}, \mathbf{I}_3)$ from a multivariate normal distribution, $C_4 \sim Unif(-3, 3)$ from a continuous uniform distribution, and one categorical variable $C_5 \sim V(-2, 2)$ from a discrete uniform distribution. We generate the unit-level surrogate $Z^* \sim N(0, 1)$ and the cluster-level surrogate $U \sim Unif(-3, 0)$, independently from other covariates.

Z , the true confounder variable, is constructed such that its distribution varies based on U and to ensure that Z^* is rank-preserving function of Z within levels of U . First, we assume that $Z|U = u \sim N(1.5u, 0.6^2)$. Then, for each sample $j = 1, \dots, N$, we assign z_j so that the probability of $Z \leq z_j$ is equal to the probability of $Z^* \leq z_j^*$, i.e., $P(Z^* \leq z_j^*; Z^* \sim N(0, 1)) = P(Z \leq z_j; Z \sim N(1.5u_j, 0.6^2))$ as illustrated in Figure 3.

We generate exposure, W , based on the GPS model with pre-exposure covariates \mathbf{C} as well as

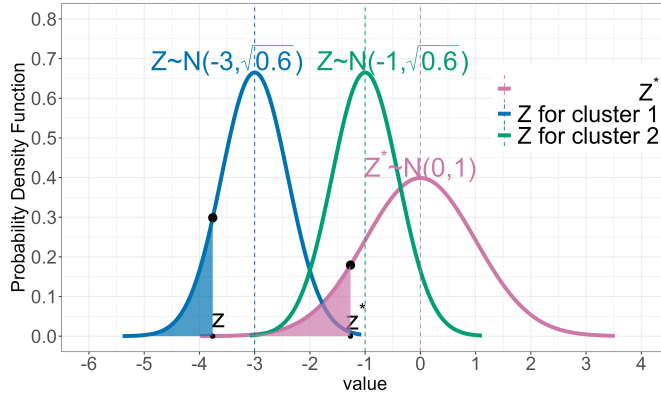


Figure 3: Illustration of the simulation procedures for Z^* and Z . In this illustration, we generate a total sample size of $N = 10,000$ with two equal sized clusters $G = 2$. We assume $Z^* \sim N(0, 1)$ and $Z|U = u \sim N(1.5u, 0.6^2)$ where $U = -2$ for cluster 1 and $U = -0.66$ for cluster 2. For each sample $j = 1, \dots, N$, we generate z_j such that the probability of $Z \leq z_j$ is equal to the probability of probability of $Z^* \leq z_j^*$, i.e., $P(Z^* \leq z_j^*; Z^* \sim N(0, 1)) = P(Z \leq z_j; Z \sim N(1.5u_j, 0.6^2))$.

the true Z , i.e.,

$$W = 11 * (-0.8 + 0.1C_2 - 0.1C_3 + 0.2C_4 + 0.1C_5 + 0.1C_6 + 0.1Z) + 21 + N(0, 5^2).$$

To emulate the $PM_{2.5}$ exposure range observed in our data application, we set the scale parameter of the exposure variable W to a constant value of 11 and the intercept to 21, ensuring that the [5%, 95%] percentiles of W are approximately equal to [0, 20]. We generate outcome Y from an outcome model specified as a cubic function of W with confounding and/or effect modification by Z . Explicitly, we let $Y | W, \mathbf{C}, Z \sim N\{\mu(W, \mathbf{C}, Z), 10^2\}$, where

$$\mu(W, \mathbf{C}, Z) = -1 - (2, 3, -1, 2, 2)\mathbf{C} - \beta_Z Z - W(0.1 + 0.1C_4 + 0.1C_5 + 0.1C_3^2 + \beta_{WZ}Z^2) + 0.13^2W^3.$$

We consider various simulations to incorporate plausible scenarios in real applications. In Scenario 1, we consider $G = 10$ equally sized clusters (i.e. balanced cluster size) with relatively large cluster size $N_g = 200$. In Scenario 2, we consider $G = 50$ equally size clusters with relatively small cluster size $N_g = 40$. In Scenario 3, we consider $G = 10$ clusters with varying cluster size (i.e. unbalanced cluster size) where cluster size N_g ranging from 14 to 422.

Within each scenario, we obtain differing confounding and effect modification structures by varying (β_Z, β_{WZ}) , where β_Z represents the influence of Z on the outcome Y , and β_{WZ} represents the effect modifying influence of Z . When β_Z is equal to zero, then it implies no confounding due

to Z . When β_{WZ} is equal to zero, it implies no effect modification due to Z . We consider all pairwise combinations of $\beta_Z = [0, 2, 4]$, and $\beta_{WZ} = [0, 0.2, 0.4]$, creating 9 different cases. For each case, we generate $S = 500$ simulated datasets.

In each simulated dataset, we calculate the true ERF empirically by taking an expectation of Y at pre-defined exposure levels $W^* = (0, 1, \dots, 19, 20)$. We use the true coefficient β 's, expectation of \mathbf{C} , and sample expectation of Z to account for variability across clusters:

$$E(Y|W^*) = -1 - \beta_Z \hat{E}[Z] - W^* (0.2 + \beta_{WZ} \hat{E}[Z^2]) + 0.13^2 W^{*3}$$

where $\hat{E}[Z] = \sum_{j=1}^N Z_j / N$ and $\hat{E}[Z^2] = \sum_{j=1}^N Z_j^2 / N$.

3.2 Competing methods and methods implementation

To our knowledge, no studies to date have attempted to estimate causal ERFs in a setting with clustered data and surrogate variables. However, here we formalize several simple adaptations of traditional GPS matching that might naturally be adopted in this setting, which will serve as competing methods in our simulation studies. Each of these approaches uses a different GPS model specification but then implements GPS matching method (Wu et al., 2022).

The first two competing approaches use Z_j^* in the GPS model but not U . The first approach, called the *unadjusted* approach, uses a GPS model that only adjusts for observed unit-level covariates \mathbf{C} and Z^* , while ignoring U and the clustering structure of the data entirely. The second approach, called the *fixed* approach, emulates a scenario where the values of U are not known exactly but the clustering structure is known, i.e., we know the sets of states that have the same U value (in our motivating example, clusters are sets of states with the same Medicaid eligibility threshold). In the *fixed* approach, the GPS model includes \mathbf{C} and cluster membership indicators (also known as “fixed effects”), denoted by R . In the third competing approach, the *adjusted* approach, the GPS model includes \mathbf{C} , Z^* , and U . The *adjusted* approach will only encourage matched units to have the same U 's if U is associated with exposure (King and Nielsen, 2019; Yang, 2018), while *MedMatch* will encourage, but not force, matching within levels of U regardless of whether U influences exposure. The GPS model specifications for *unadjusted*, *fixed*, and *adjusted* are as

follows:

$$\begin{aligned}
\text{unadjusted: } e(w, \mathbf{c}) &= f_{W_j | \mathbf{C}_j, Z_j^*}(w | \mathbf{c}, z^*), \\
\text{fixed: } e(w, \mathbf{c}, r) &= f_{W_j | \mathbf{C}_j, R_j}(w | \mathbf{c}, r), \\
\text{adjusted: } e(w, \mathbf{c}, u) &= f_{W_j | \mathbf{C}_j, Z_j^*, U_j}(w | \mathbf{c}, z^*, u).
\end{aligned} \tag{3}$$

We also implement *within*-cluster matching, as described in Section 2.2 and *MedMatch* as described in Section 2.3. In each approach, we estimate the GPS conditional means using a fitted extreme gradient boosting machine (GBM) implemented in the `Superlearner` R package (Chen and Guestrin, 2016; Zhu et al., 2015; Van der Laan et al., 2007). We denote average of ACs as $\rho_{\{\cdot\}}$, where \cdot represents set of adjusted covariates (e.g., average of ACs for *adjusted* is $\rho_{\{\mathbf{C}, Z^*, U\}} = \frac{\rho_{C_1} + \dots + \rho_{C_p} + \rho_{Z^*} + \rho_U}{p=2}$). To find optimal matching hyperparameters for each approach (besides *Within* matching as described below), we use a grid search and identify the hyperparameters that yield the minimum average AC. To ensure that the GPS yields covariate balance in the matched data, we also consider a range of possible hyperparameters for the GBM, such as maximum number of boosting iterations and shrinkage factors. When estimating the ERF, to avoid instability at the boundaries of the exposure range, we trim the support of W by excluding units outside of the range of [5%, 95%] percentiles of W prior to the analysis. For *within* matching, because conducting a grid search of hyperparameters for each cluster separately is too computationally expensive, we use the same hyperparameters for the GBM as selected for the *MedMatch* approach for each cluster’s matching procedure.

After implementing standard GPS matching algorithm (Wu et al., 2022) using any of the above four methods (*unadjusted*, *fixed*, *adjusted* or *within*), an assessment of covariate balance, estimation of the ERF, and uncertainty estimation can proceed as described in Section 2.3.

3.3 Measures for assessment of the performance

To assess the performance of the different methods, we calculated the absolute bias (AB) and root mean squared error (RMSE) (Kennedy et al., 2017). We first calculate the empirical AB and RMSE at each point w across simulations $s = 1, \dots, S$ and then integrate it across the range of w .

The measures are defined below:

$$\widehat{\text{Absolute Bias}} = \int_{\mathbb{W}^\dagger} \left| \frac{1}{S} \sum_{s=1}^S \hat{Y}_s(w) - Y(w) \right| f_W(w) dw,$$

$$\widehat{\text{RMSE}} = \int_{\mathbb{W}^\dagger} \left[\frac{1}{S} \sum_{s=1}^S \{ \hat{Y}_s(w) - Y(w) \}^2 \right]^{1/2} f_W(w) dw,$$

where \mathbb{W}^\dagger is a trimmed support of \mathbb{W} to avoid instability in boundaries.

Moreover, we calculate Kolmogorov–Smirnov (KS) statistic (Massey Jr, 1951) which is defined as the largest vertical statistic difference between the two empirical cumulative density function evaluated at any point. We compare the KS statistic of Z between the original data and the matched data to assess whether the target population’s distribution of Z is well preserved. The smaller the KS statistic, the closer together the two distributions under consideration.

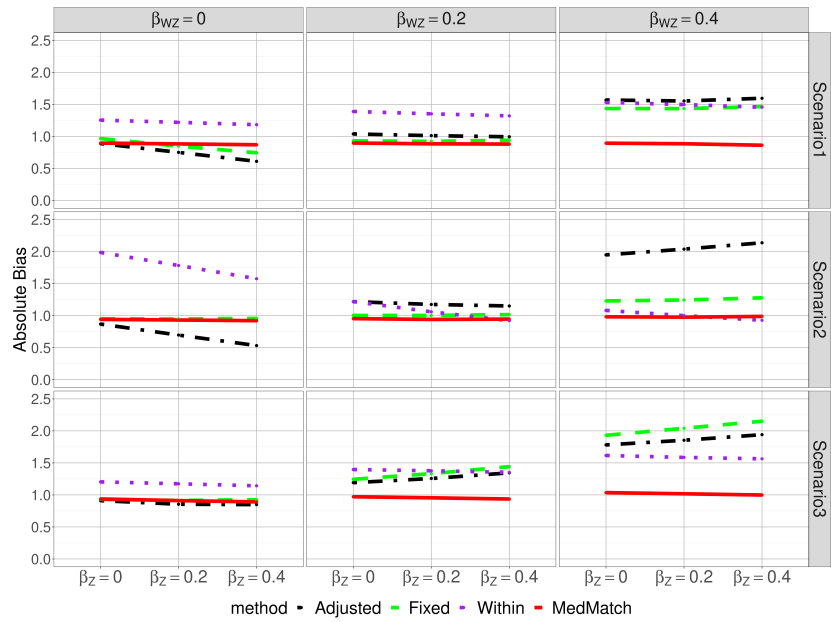
We further estimate effective sample size (ESS) in the matched data, which corresponds to ESS of a weighted sample. Suppose the j' -th unit in the s -th simulated dataset appears $n_{sj'}$ times in the matched dataset. Then, ESS is defined as (Kish, 1965)

$$\widehat{\text{ESS}} = \frac{1}{S} \sum_{s=1}^S \left\{ \frac{(\sum_{j'} n_{sj'})^2}{\sum_{j'} n_{sj'}^2} \right\}.$$

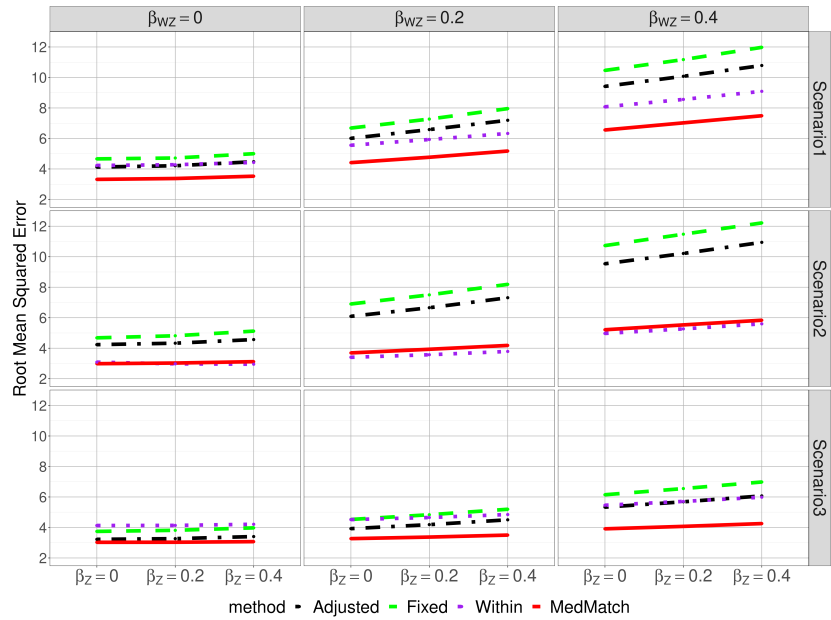
$ESS = 1$ indicates that only one unit is used as a match and it serves as the match for every other unit in the data, whereas $ESS = N$ indicates that every unit is used as a match. Thus, a small ESS would indicate the possible existence of a few very influential observations with numerous matches (Chattopadhyay et al., 2020), which is generally undesirable as it leads to a high-variance estimator.

3.4 Simulation results

AB and RMSE results for Scenarios 1, 2, and 3 are shown in Figures 4a and 4b, respectively. The results for *unadjusted* are omitted from these plots because its poor performance in many scenarios distorts the scaling of the figures. Analogous plots with the *unadjusted* results added are given in Figure S2. Figure S1 and Figure S5 presents the ESS and KS divergence for each covariate in the original vs. matched data for each method and scenario. Figure S3 and Figure S4 presents average of AC for each covariate (denoted as $\bar{\rho}_{C_1}, \dots, \bar{\rho}_{C_5}, \bar{\rho}_U, \bar{\rho}_{Z^*}, \bar{\rho}_Z$) and boxplots of $\rho_{C,Z}$ across the 500 simulated datasets in the original and matched data for each method and scenario. The optimal



(a) Absolute Bias (AB)



(b) Root Mean Squared Error (RMSE)

Figure 4: Simulation results: absolute bias (AB) and root mean square error (RMSE) of the *adjusted* (black dot dashed line), *fixed* (green dashed line), *within* (purple dotted line) and *MedMatch* (red solid line) methods across 500 simulations. The simulated data are composed of $G = 10$ equally sized clusters in Scenario 1; $G = 50$ equally sized clusters in Scenario 2; and $G = 10$ clusters with varying cluster size in Scenario 3. β_Z and β_{WZ} represent the strength of confounding and effect modification by Z , respectively. The results for the *unadjusted* method are omitted here to avoid plot scale distortions (see Figure S2).

hyperparameters for each method and scenario are given in Table S1. Some consistent patterns can be observed across all three scenarios, which are described below.

First, we highlight general takeaways from the AB results. When confounding and/or effect modification by Z is present, approaches that account for the clustering structure, either through directly adjusting for U or using cluster fixed effects (*MedMatch*, *within*, *adjusted*, and *fixed*) tend to give smaller AB than the *unadjusted* approach, which ignores the clustering (Figure S2). This is likely due to imbalance in Z and U across exposure levels in the matched data as the $\bar{\rho}_Z, \bar{\rho}_U > 0.1$ (Figure S3). The worse AB of *unadjusted* compared to the other methods grows especially pronounced as the strength of both confounding and effect modification increase. In the rest of the section, we ignore *unadjusted* in our comparisons due to its poor AB performance.

The strength of effect modification by Z (size of β_{WZ}) impacts the relative performance of the methods more than the strength of confounding by Z (size of β_Z). The AB of *adjusted*, *within*, and *fixed* tend to increase as the strength of effect modification increases, while the AB of *MedMatch* remains small and nearly constant across all scenarios and confounding/effect modification structures (Figure 4a). This may be partly explained by the fact that covariate balance is always achieved (i.e., $\rho_{\{C,Z\}} < 0.1$) for *MedMatch* whereas the other methods often did not attain covariate balance (Figure S4). In addition, the KS distance of Z in the original vs matched data is generally smaller when using *MedMatch* compared to the other methods (Figure S5). This indicates that *MedMatch* better preserves the target population’s distribution of Z , in spite of not directly using Z in the estimation.

Second, we highlight consistent patterns in the RMSE results (Figure 4b). *MedMatch* always yields the smallest RMSE among all the methods in Scenarios 1 and 3. This is likely because *MedMatch* typically has the largest ESS (Figure S1) and therefore the lowest variance, and it generally has the smallest AB among the methods as well.

Finally, in the presence of effect modification by Z ($\beta_{WZ} \neq 0$), *MedMatch* always out-performs the other methods in terms of both AB and RMSE. This can be at least partly explained by the smaller KS distance of Z in the original vs matched data when using *MedMatch* compared to the other methods, on top of achieving covariate balance (Figure S5). This indicates that *MedMatch* better preserves the target population’s distribution of Z , in spite of not directly using Z in the estimation. In fact, *MedMatch* has the smallest KS for all covariates compared to other methods in Scenario 1 and 3.

Comparing the results across scenarios provides insight into how cluster number, within-cluster sample size, and cluster balance impact the relative performance of the methods. We assess the impact of large or small cluster sample size in the balanced case by comparing Scenarios 1 and 2 (Figure 4). The performance of *within* matching changes most notably across Scenarios 1 and 2, and contrary to expectation, its relative performance (in terms of both AB and RMSE) is generally better in Scenario 2 than Scenario 1. In Scenario 2, *within* even out-performs *MedMatch* in some settings. This is due to the much larger ESS of *within* in Scenario 2 (Figure S1), which occurs because it forces matches within the small clusters, resulting in a more diverse set of units being used as matches and therefore limiting the opportunity for a few observations to have extreme influence. In Scenario 2, the AB of *within* is largest when effect modification by Z is not present ($\beta_{WZ} = 0$), likely due to imbalance in covariates \mathbf{C} and therefore residual confounding in the matched data (Figure S3). However, as the strength of effect modification by Z (size of β_{WZ}) increases, the AB of *within* decreases. This is likely because balancing Z becomes more important, compared to \mathbf{C} , as β_{WZ} increases, and *within* tends to achieve balance on Z .

Furthermore, we assess the impact of unbalanced cluster sizes by comparing Scenario 3 to 1 (Figure 4). Relative to Scenario 1, in Scenario 3 the AB of *fixed* generally increases, whereas the AB of the other methods remain relatively unaffected. This may be because the presence of some very small clusters leads to instability in the GPS model with fixed effects. The RMSE of all the methods are generally smaller in Scenario 3 than Scenario 1, due to generally higher ESS's in Scenario 3 (Figure S1). Thus, on the whole, having balanced clusters does not seem to be advantageous for causal ERF estimation in clustered data.

In summary, through simulation studies, we have shown that *MedMatch* generally outperforms other possible extensions of existing methods in estimation of a population-level ERF in data structured to mimic features of the real Medicaid and $PM_{2.5}$ data. Moreover, we show its robustness to the number of clusters, cluster sizes, and varying strength of confounding and effect modifying influence of the unmeasured Z variable.

4 PM_{2.5} and Childhood Respiratory Outcomes in Medicaid

4.1 Data description

Our study includes 23.4 million children ages 6-18 enrolled in Medicaid sometime during the period 2000-2012 and living in 46 states in the continental US and Washington DC. Among the 48 contiguous US states, we exclude Kansas and Maine because Medicaid claims data for Maine from 2005-2010 and Kansas for 2010 are unavailable. Each beneficiary’s self-reported zip code of residence, state of Medicaid enrollment, age, race and sex are provided in the enrollment files. We use international classification of diseases (ICD) codes to identify inpatient hospitalizations where the primary or secondary cause is diseases the respiratory system (ICD-9: 460-519) which includes pneumonia, influenza, acute respiratory infections, etc. We include only the first respiratory hospitalization for the enrollees who experienced multiple hospitalizations during the study period. We aggregate the individual-level data to the zip code level for each year to calculate respiratory hospitalization rate. Specifically, for each zip code and year, we divide the number of respiratory hospitalizations by the corresponding total person-years of follow-up in the zip code and use this rate as the outcome in our analyses.

We utilize the same zip code level annual PM_{2.5} concentrations and potential confounders employed in several high-impact studies of the health effects of PM_{2.5} in the Medicare population (Di et al., 2017; Wu et al., 2022, 2020; Wei et al., 2022). In brief, we obtain daily predictions of PM_{2.5} exposures at the centroids of a 1-km² grid covering the continental US using an ensemble-based prediction model (Di et al., 2019), which has been shown to have a cross-validated R² of 0.86. We average the daily PM_{2.5} exposure predictions across grid cells within the boundary of each zip code and across the days within each year to obtain annual average PM_{2.5} exposures, which are linked with the Medicaid data by zip code (Wu et al., 2022, 2020; Wei et al., 2022). We consider 18 possible zip code level confounders such as socio-demographic, health behavior, and meteorological variables collated from various sources explained in Section S.2.1.

Moreover, we obtain publicly available state-level Medicaid family income eligibility threshold as a percent of the federal poverty level (%FPL) for age group 6-18 provided for each year (Brooks et al., 2019). In summary, although our data include 46 states and Washington DC, some states have same eligibility threshold, resulting in only 10 unique Medicaid eligibility thresholds (%FPL = 100, 133, 140, 150, 185, 200, 235, 250, 275, 300). This creates 10 clusters. Many clusters never

experience extreme $\text{PM}_{2.5}$ concentrations falling in the tails of the distribution (Figure S6), so that only a few clusters are represented in the far lower and upper tails of the $\text{PM}_{2.5}$ distribution. Thus, to avoid violations of the positivity assumption, we only include units (zip code-years) with observed exposures within the subset of the exposure range where at least 7 out of the 10 clusters are represented (Figure S6). This includes units with annual average $\text{PM}_{2.5}$ values within the range of $2.92 - 13.27 \mu\text{g}/\text{m}^3$. A detailed description of the data cleaning procedures can be found in Section S.2.1. In summary, our final analytic data contain a total of 249,167 zip code-years (with $n = 28,477$ unique zip codes).

4.2 Data analysis

To apply *MedMatch* on the real data, we first estimate the surrogate GPS using a GBM and including all the confounders listed above as predictors. To ensure covariate balance in the matched data produced by *MedMatch*, we search a grid of hyperparameters (δ, τ) with two candidate calipers $\delta = (0.61, 0.30)$ (corresponding to $L = 50, 100$) and ten candidate scale parameters $\tau = (0.1, 0.2, 0.3, \dots, 0.9, 1)$. We found that the combination of hyperparameters that minimize the average AC $\rho_{\{\mathbf{C}, Z^*, U\}}$ were $(\delta, \tau) = (0.61, 0.8)$. *MedMatch* resulted in significant improvement in the covariate balance of the majority of covariates in the matched data relative to the original data (Figure S8). Prior to matching, there were 10 covariates with $\text{AC} > 0.1$, with a maximum AC equal to 0.31, but after matching, only four covariates had AC above 0.1 with a maximum AC of 0.13. Furthermore, the average AC improved from 0.14 prior to matching to 0.06 after matching.

After matching, we estimate the causal ERF of long term $\text{PM}_{2.5}$ exposure and respiratory hospitalization rate by fitting a kernel smoother with Gaussian kernel on the entire matched dataset. We use the block m-out-of-n bootstrap procedure as described in Section 2.4 to construct a point-wise Wald 95% confidence band for the ERF. Specifically, for each re-sampling, we include all zip code-years associated with sampled zip codes to account for the across-year correlation. We sample $m = 2\sqrt{n} \approx 337$ zip codes with replacement and we ensure that each cluster is adequately represented by sampling a fixed number of units from each cluster, proportional to its representation in the original dataset.

Figure 5 shows the estimated average causal ERF relating long-term $\text{PM}_{2.5}$ exposure to respiratory hospitalization rate (left) and the associated hazard ratios (right). To calculate the hazard ratio, we divide the outcome rate at each exposure level by the baseline rate, which is the estimated

average outcome rate at the minimum $\text{PM}_{2.5}$ exposure value in the data (i.e. $2.92 \mu\text{g}/\text{m}^3$). We find a harmful effect of long-term $\text{PM}_{2.5}$ exposure on respiratory hospitalization rate in Medicaid children, as indicated by the increasing ERFs. Specifically, the curve is steeper at $\text{PM}_{2.5} \leq 8 \mu\text{g}/\text{m}^3$ and starts to level off at higher concentrations. The slight downturn in the right tail has large associated uncertainty and may be due to the smaller number of clusters represented, and therefore potential violations of the positivity assumption, at higher $\text{PM}_{2.5}$ levels. We also compare the causal ERF estimated using the *MedMatch* to *adjusted* (Figure S9). The *adjusted* ERF shows sharper increases in respiratory hospitalization rate as $\text{PM}_{2.5}$ increases compared to *MedMatch*, such that the respiratory hospitalization rate at $\text{PM}_{2.5}=11.1 \mu\text{g}/\text{m}^3$ is 4.1 times higher than the baseline rate, compared to 2.4 times higher for *MedMatch* (Figure S9).

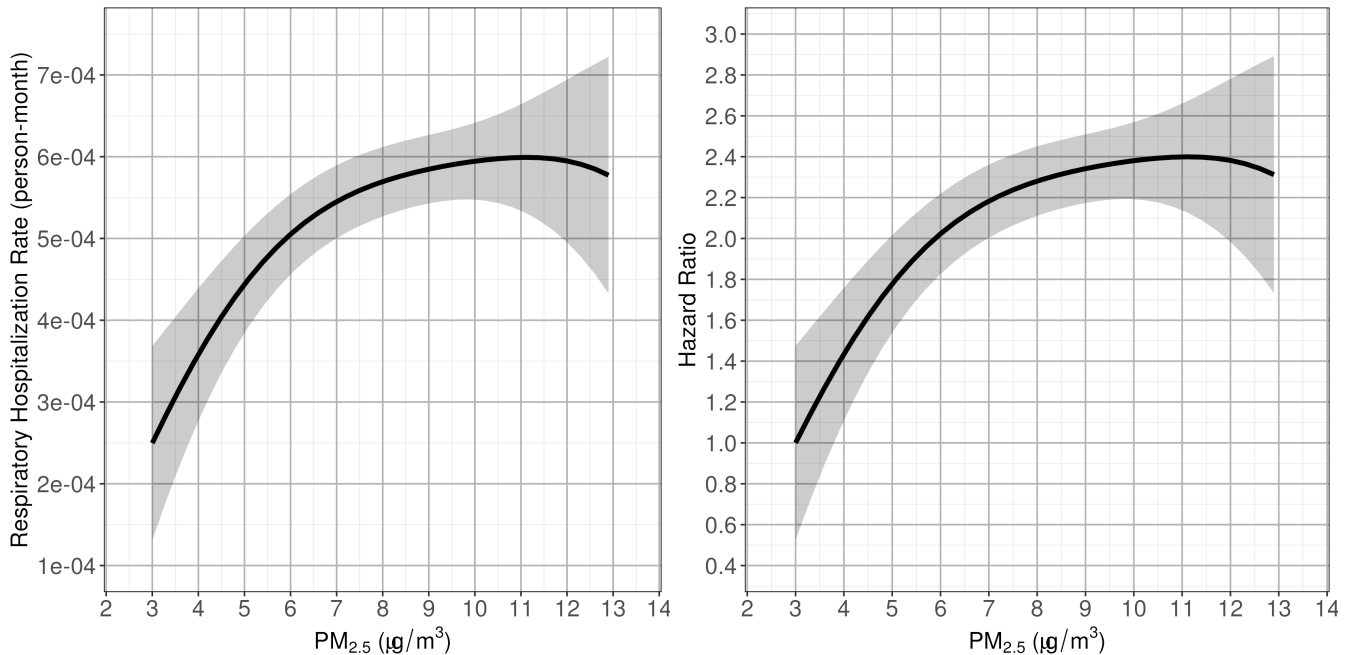


Figure 5: The *MedMatch* estimated causal ERF relating respiratory hospitalization to long-term $\text{PM}_{2.5}$ exposure in children enrolled in Medicaid (2000-2012). The shaded area represent the point-wise Wald 95% confidence band, with standard errors calculated by block m-out-of-n bootstrap.

5 Discussion

In this paper, we proposed a causal inference method called *MedMatch* to address challenges to estimating ERFs of environmental exposures on health outcomes using nationwide Medicaid claims data. *MedMatch* accounts for the following unique features of nationwide children’s Medicaid claims

and environmental exposure data: 1) the health outcome data have a clustering structure due to differing income-based Medicaid eligibility thresholds by state, 2) MHI-MC, an important potential confounder and effect modifier, is unmeasured, and 3) two surrogate variables are measured, zip code median household income and state eligibility threshold. Median household income was posited to be a rank-preserving function of MHI-MC, conditional on Medicaid eligibility threshold. Through simulation studies, we demonstrated that, under the requisite assumptions, *MedMatch* is able to recover the population average causal ERF with little bias using the surrogate measures, and it consistently out-performs competing alternative approaches under a range of scenarios. The benefits of *MedMatch* were most pronounced when the unmeasured variable is an effect modifier and a confounder, which is known to be the case for our income and air pollution motivating example.

We applied *MedMatch* to estimate the causal ERF of long-term $\text{PM}_{2.5}$ exposure on first respiratory hospitalization in Medicaid children enrollees of age 6-18 between 2000 and 2012. Three previous studies used nationwide Medicaid data to study associations between $\text{PM}_{2.5}$ exposure and health. Like ours, these studies found positive associations. In particular, they reported positive associations between short-term $\text{PM}_{2.5}$ and cardiovascular and asthma hospitalizations in adults (Wei et al., 2022; deSouza et al., 2021) and between long-term $\text{PM}_{2.5}$ and asthma in children (Keet et al., 2018). Most other studies using Medicaid data have focused on single cities only and on short-term $\text{PM}_{2.5}$ exposure (Li et al., 2011; Wendt et al., 2014; Mann et al., 2010). To our knowledge, no previous studies have examined the ERF of long-term $\text{PM}_{2.5}$ exposure and respiratory hospitalization in children in Medicaid nationwide using a causal inference approach. Moreover, none of these papers has tackled the methodological challenges associated with the geographically-varying enrollment criteria for Medicaid, which generates a unique clustering structure in the data.

There are several strengths of the proposed method. First, the proposed method enables estimation of the population average causal ERF in the presence of an unmeasured confounder and/or effect modifier. Second, implementation of within-cluster matching approaches requires significant manual tuning and is computationally burdensome (e.g. one must estimate the GPS model and optimize hyperparameters separately for each cluster, within each cluster, etc), whereas *MedMatch* requires estimation of only a single GPS model and selection of only one set of hyperparameters. Third, compared to previously proposed matching methods for clustered data (Arpino and Cannas, 2016; Rickles and Seltzer, 2014), which require defining an arbitrary threshold to decide whether a

candidate within-cluster match is “appropriate”, the proposed method instead enables selection of the weight τ for the proposed matching method through a data-driven approach. Fourth, the proposed matching method is not confined to clustered observational data but can also be extended to adjust for unmeasured spatial confounding by replacing U in the matching function with a variable that measures spatial proximity, as Papadogeorgou et al. (2019) proposed in the binary treatment setting.

There are also several limitations of our analyses that could be addressed in future work. First, *MedMatch* assumes units in a cluster share a common eligibility threshold largely based on income level. To extend the analysis to the entire Medicaid population, which includes children, parents, pregnant woman, and disabled adults and where each group has different eligibility criteria, further methods development may be needed. Second, we used m-out-of-n bootstrapping to calculate Wald confidence band of the causal ERF. A recent paper proposed causal ERF estimation using Gaussian processes, which not only enable automatic uncertainty evaluation but also enable change point detection through inference on derivatives of the ERF (Ren et al., 2021). Future research could incorporate the ideas developed here into a Gaussian process framework. Third, although our assumption that Z^* is a rank-preserving function of Z is expected to be roughly met in our data application, it is likely not strictly true and is not testable. Fourth, $PM_{2.5}$ concentrations are measured only at centrally located monitors, necessitating the use of model-based $PM_{2.5}$ exposure predictions. These are subject to exposure measurement error; however, Josey et al. (2023) show that the measurement error in the predictions used here do not significantly impact causal ERF estimates. Fifth, because pollution sources at one location affect pollution and health at other locations, SUTVA may be violated in these data. Future research in the setting of exposure measurement error and/or interference may be interesting.

Acknowledgements

This work was supported by NIH grants T32ES007142 and K01ES032458, the Harvard Data Science Initiative, and the Harvard Global Health Institute Burke Climate and Health Fellowship, in collaboration with the Salata Institute for Climate and Sustainability at Harvard University.

The computations in this paper were run on the FASRC Cannon cluster supported by the FAS Division of Science Research Computing Group at Harvard University.

Data and code availability

Code to reproduce all simulation studies and real data analyses is available at <https://github.com/jennyjyounglee/MedMatch>. The Medicaid claims data used here can be obtained upon request and approval from the US Centers for Medicare and Medicaid Services. PM_{2.5} data are publicly available at <https://doi.org/10.7927/9yp5-hz11>, and confounder data are publicly available from the US Census Bureau, Gridmet, and the US CDC. State-specific Medicaid eligibility threshold data are available on the Kaiser Family Foundation website at <https://www.kff.org/state-category/medicaid-chip/trends-in-medicaid-income-eligibility-limits/>.

References

- Arpino, B. and Cannas, M. (2016). Propensity score matching with clustered data. an application to the estimation of the impact of caesarean section on the apgar score. *Statistics in medicine*, 35(12):2074–2091.
- Brooks, T., Roygardner, L., Artiga, S., Pham, O., and Dolan, R. (2019). Medicaid and chip eligibility, enrollment, and cost sharing policies as of january 2019: Findings from a 50-state survey. *San Francisco: Kaiser Family Foundation*. Accessed January, 22:2020.
- Cakmak, S., Hebborn, C., Cakmak, J. D., and Vanos, J. (2016). The modifying effect of socioeconomic status on the relationship between traffic, air pollution and respiratory health in elementary schoolchildren. *Journal of Environmental Management*, 177:1–8.
- Chattopadhyay, A., Hase, C. H., and Zubizarreta, J. R. (2020). Balancing vs modeling approaches to weighting in practice. *Statistics in Medicine*, 39(24):3227–3254.
- Chen, T. and Guestrin, C. (2016). Xgboost: A scalable tree boosting system. In *Proceedings of the 22nd acm sigkdd international conference on knowledge discovery and data mining*, pages 785–794.
- Cork, M., Mork, D., and Dominici, F. (2023). Methods for estimating the exposure-response curve to inform the new safety standards for fine particulate matter. *arXiv preprint arXiv:2306.03011*.
- Cortes-Ramirez, J., Wilches-Vega, J. D., Paris-Pineda, O. M., Rod, J., Ayurzana, L., and Sly,

- P. D. (2021). Environmental risk factors associated with respiratory diseases in children with socioeconomic disadvantage. *Heliyon*, 7(4):e06820.
- deSouza, P., Braun, D., Parks, R. M., Schwartz, J., Dominici, F., and Kioumourtzoglou, M.-A. (2021). Nationwide study of short-term exposure to fine particulate matter and cardiovascular hospitalizations among medicaid enrollees. *Epidemiology (Cambridge, Mass.)*, 32(1):6.
- Di, Q., Amini, H., Shi, L., Kloog, I., Silvern, R., Kelly, J., Sabath, M. B., Choirat, C., Koutrakis, P., Lyapustin, A., et al. (2019). An ensemble-based model of pm2.5 concentration across the contiguous united states with high spatiotemporal resolution. *Environment International*, 130:104909.
- Di, Q., Wang, Y., Zanobetti, A., Wang, Y., Koutrakis, P., Choirat, C., Dominici, F., and Schwartz, J. D. (2017). Air pollution and mortality in the medicare population. *New England Journal of Medicine*, 376(26):2513–2522.
- Greenland, S., Pearl, J., and Robins, J. M. (1999). Confounding and collapsibility in causal inference. *Statistical science*, 14(1):29–46.
- Hajat, A., MacLehose, R. F., Rosofsky, A., Walker, K. D., and Clougherty, J. E. (2021). Confounding by socioeconomic status in epidemiological studies of air pollution and health: challenges and opportunities. *Environmental health perspectives*, 129(6):065001.
- Hirano, K. and Imbens, G. W. (2004). The propensity score with continuous treatments. *Applied Bayesian modeling and causal inference from incomplete-data perspectives*, 226164:73–84.
- Josey, K. P., DeSouza, P., Wu, X., Braun, D., and Nethery, R. (2023). Estimating a causal exposure response function with a continuous error-prone exposure: a study of fine particulate matter and all-cause mortality. *Journal of Agricultural, Biological and Environmental Statistics*, 28(1):20–41.
- Keet, C. A., Keller, J. P., and Peng, R. D. (2018). Long-term coarse particulate matter exposure is associated with asthma among children in medicaid. *American journal of respiratory and critical care medicine*, 197(6):737–746.
- Kennedy, E. H., Ma, Z., McHugh, M. D., and Small, D. S. (2017). Non-parametric methods for doubly robust estimation of continuous treatment effects. *Journal of the Royal Statistical Society: Series B (Statistical Methodology)*, 79(4):1229–1245.

- Kim, J.-S. and Steiner, P. M. (2015). Multilevel propensity score methods for estimating causal effects: A latent class modeling strategy. In *Quantitative psychology research*, pages 293–306. Springer.
- King, G. and Nielsen, R. (2019). Why propensity scores should not be used for matching. *Political analysis*, 27(4):435–454.
- Kish, L. (1965). Survey sampling.
- Li, S., Batterman, S., Wasilevich, E., Wahl, R., Wirth, J., Su, F.-C., and Mukherjee, B. (2011). Association of daily asthma emergency department visits and hospital admissions with ambient air pollutants among the pediatric medicaid population in detroit: time-series and time-stratified case-crossover analyses with threshold effects. *Environmental research*, 111(8):1137–1147.
- Mann, J. K., Balmes, J. R., Bruckner, T. A., Mortimer, K. M., Margolis, H. G., Pratt, B., Hammond, S. K., Lurmann, F. W., and Tager, I. B. (2010). Short-term effects of air pollution on wheeze in asthmatic children in fresno, california. *Environmental health perspectives*, 118(10):1497–1502.
- Massey Jr, F. J. (1951). The kolmogorov-smirnov test for goodness of fit. *Journal of the American statistical Association*, 46(253):68–78.
- Papadogeorgou, G., Choirat, C., and Zigler, C. M. (2019). Adjusting for unmeasured spatial confounding with distance adjusted propensity score matching. *Biostatistics*, 20(2):256–272.
- Ren, B., Wu, X., Braun, D., Pillai, N., and Dominici, F. (2021). Bayesian modeling for exposure response curve via gaussian processes: Causal effects of exposure to air pollution on health outcomes. *arXiv preprint arXiv:2105.03454*.
- Rickles, J. H. and Seltzer, M. (2014). A two-stage propensity score matching strategy for treatment effect estimation in a multisite observational study. *Journal of Educational and Behavioral Statistics*, 39(6):612–636.
- Rubin, D. B. (1974). Estimating causal effects of treatments in randomized and nonrandomized studies. *Journal of Educational Psychology*, 66(5):688.

- Rubin, D. B. (1980). Randomization analysis of experimental data: The fisher randomization test comment. *Journal of the American statistical association*, 75(371):591–593.
- Thoemmes, F. J. and West, S. G. (2011). The use of propensity scores for nonrandomized designs with clustered data. *Multivariate Behavioral Research*, 46(3):514–543.
- Truffer, C. J., Klemm, J. D., Wolfe, C. J., Rennie, K. E., and Shuff, J. F. (2016). actuarial report on the financial outlook for medicaid. *Office of the Actuary Centers for Medicare and Medicaid Services, Department of Health and Human Services*.
- Van der Laan, M. J., Polley, E. C., and Hubbard, A. E. (2007). Super learner. *Statistical applications in genetics and molecular biology*, 6(1).
- VanderWeele, T. J. and Robins, J. M. (2007). Four types of effect modification: a classification based on directed acyclic graphs. *Epidemiology*, 18(5):561–568.
- Wei, Y., Qiu, X., Sabath, M. B., Yazdi, M. D., Yin, K., Li, L., Peralta, A. A., Wang, C., Koutrakis, P., Zanobetti, A., et al. (2022). Air pollutants and asthma hospitalization in the medicaid population. *American Journal of Respiratory and Critical Care Medicine*, 205(9):1075–1083.
- Wendt, J. K., Symanski, E., Stock, T. H., Chan, W., and Du, X. L. (2014). Association of short-term increases in ambient air pollution and timing of initial asthma diagnosis among medicaid-enrolled children in a metropolitan area. *Environmental research*, 131:50–58.
- World Health Organization (2018). Air pollution and child health: prescribing clean air. Geneva: World Health Organization; 2018 (WHO/CED/PHE/18.01). Licence: CC BY-NC-SA 3.0 IGO. <https://www.who.int/publications/i/item/air-pollution-and-child-health>.
- Wu, X., Braun, D., Schwartz, J., Kioumourtzoglou, M., and Dominici, F. (2020). Evaluating the impact of long-term exposure to fine particulate matter on mortality among the elderly. *Science advances*, 6(29):eaba5692.
- Wu, X., Mealli, F., Kioumourtzoglou, M.-A., Dominici, F., and Braun, D. (2022). Matching on generalized propensity scores with continuous exposures. *Journal of the American Statistical Association*, (just-accepted):1–28.

Yang, S. (2018). Propensity score weighting for causal inference with clustered data. *Journal of Causal Inference*, 6(2).

Zhu, Y., Coffman, D. L., and Ghosh, D. (2015). A boosting algorithm for estimating generalized propensity scores with continuous treatments. *Journal of causal inference*, 3(1):25–40.

S Supplementary Materials

S.1 Simulations: Tables and Figures

Table S1: Optimal hyperparameters for caliper and scale.

(caliper,scale)	Adjusted	Unadjusted	Fixed	Within	MedMatch
Scenario 1	(0.4,0.1)	(0.2,1)	(0.6,0.2)	(1.5,1)	(2,0.3)
Scenario 2	(0.5,0.3)	(0.4,0.4)	(0.8,0.6)	(2,0.4)	(1,0.4)
Scenario 3	(0.2,0.9)	(0.3,1)	(0.3,0.5)	(1.1,0.2)	(0.9,0.2)

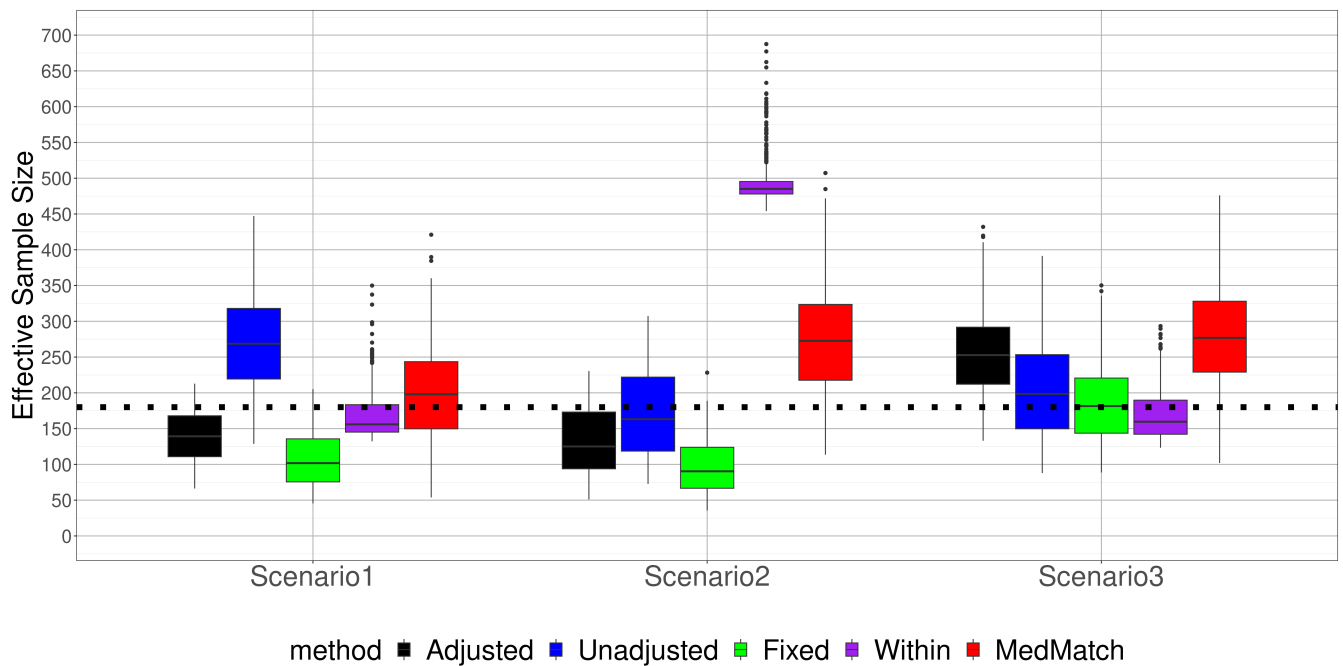
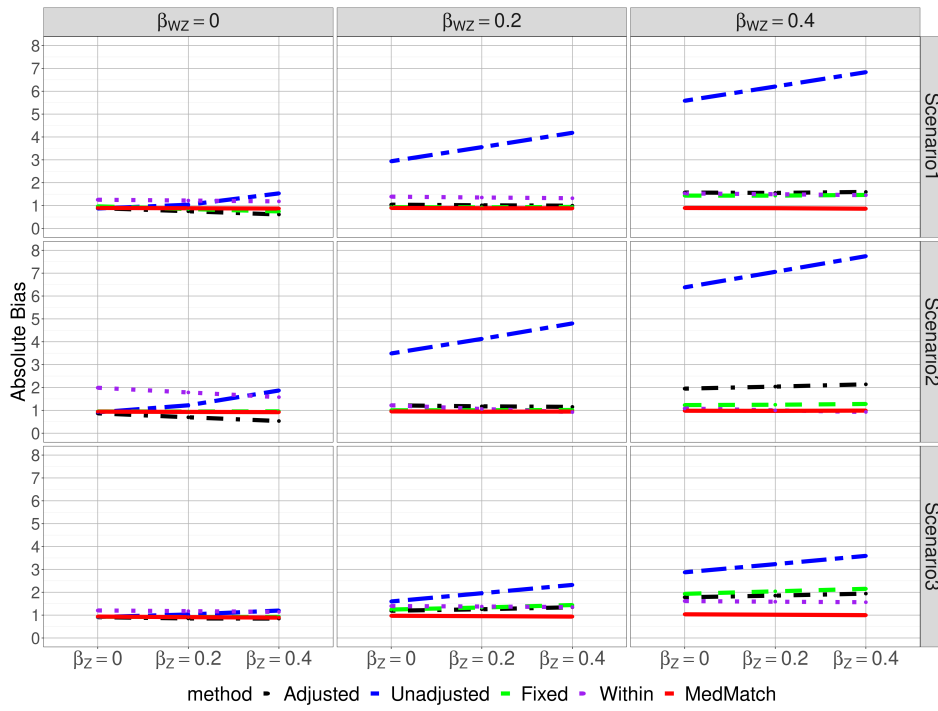
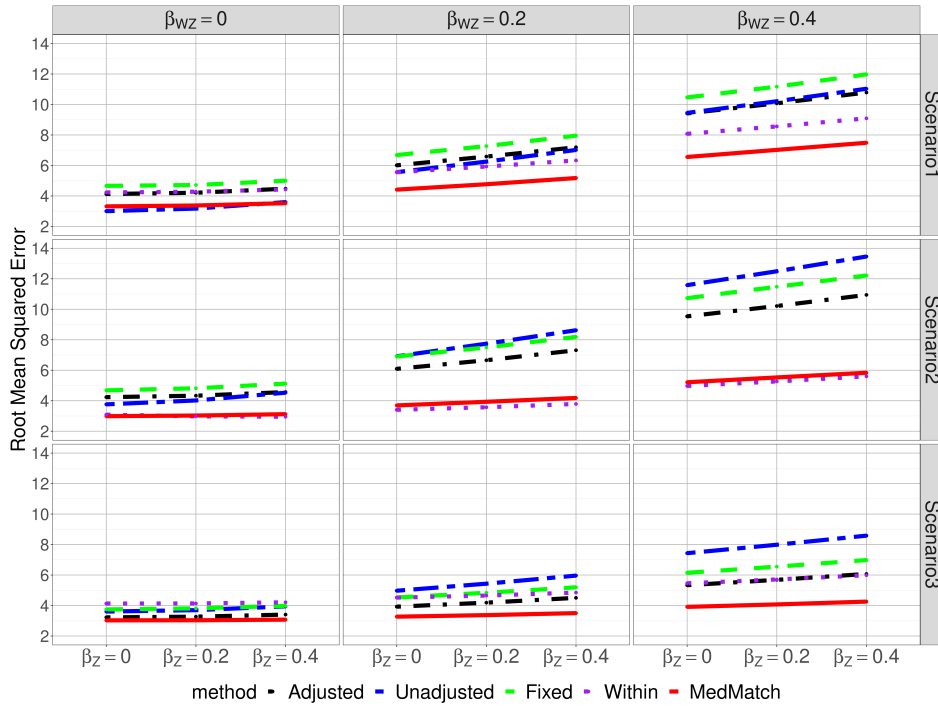


Figure S1: Boxplots of ESS across 500 simulations for each method and each scenario. A black dotted line is a minimum recommended ESS at 180 which is 10% of the $N = 2,000$ after trimming the data outside of the exposure range of [5%, 95%].



(a) Absolute Bias (AB)



(b) Root Mean Squared Error (RMSE)

Figure S2: Simulation results: absolute bias (AB) and root mean square error (RMSE) of the *adjusted* (black dot dashed line), *fixed* (green dashed line), *within* (purple dotted line) and *MedMatch* (red solid line) methods across 500 simulations. We consider $G = 10$ equally sized clusters in Scenario 1; $G = 50$ equally size clusters in Scenario 2; and $G = 10$ clusters with varying cluster size of $N_g = 14, 21, 67, 105, 228, 230, 263, 317, 333,$ and 422 in Scenario 3.

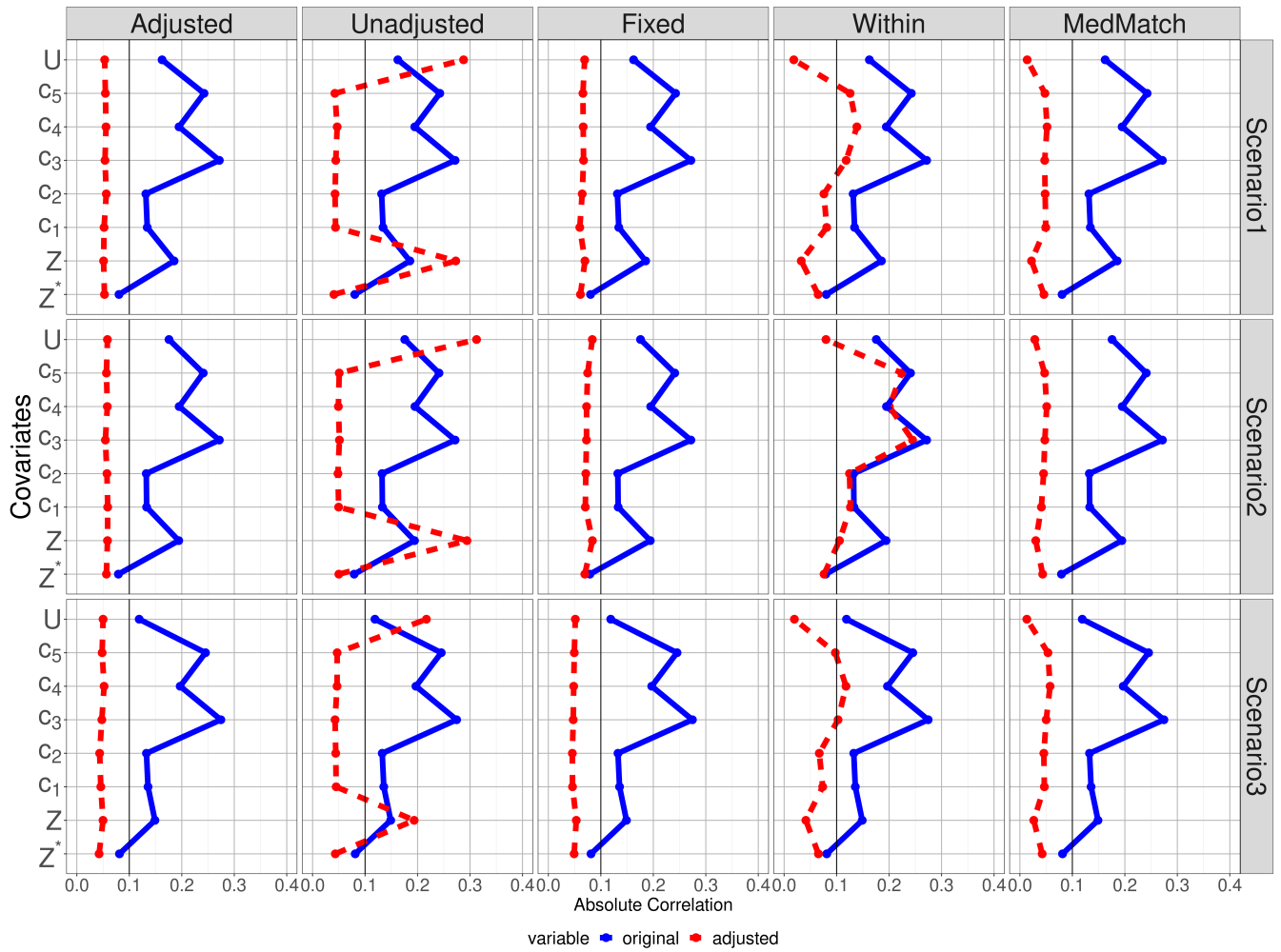


Figure S3: Simulation results: Absolute correlation for each covariate in the original dataset (blue solid line) and matched dataset (red dotted line) averaged across 500 simulated datasets (i.e., $\bar{\rho}_{C_1}, \dots, \bar{\rho}_{C_5}, \bar{\rho}_U, \bar{\rho}_{Z^*}, \bar{\rho}_Z$) for each method (columns) and scenario (rows). In the matched dataset, covariates are on average balanced across exposure levels for *adjusted*, *fixed* and *MedMatch*. However, some covariates are not balanced for *unadjusted* (i.e., $\bar{\rho}_Z, \bar{\rho}_U > 0.1$) and *within* (i.e., $\bar{\rho}_{C_3}, \bar{\rho}_{C_4}, \bar{\rho}_{C_5} > 0.1$).

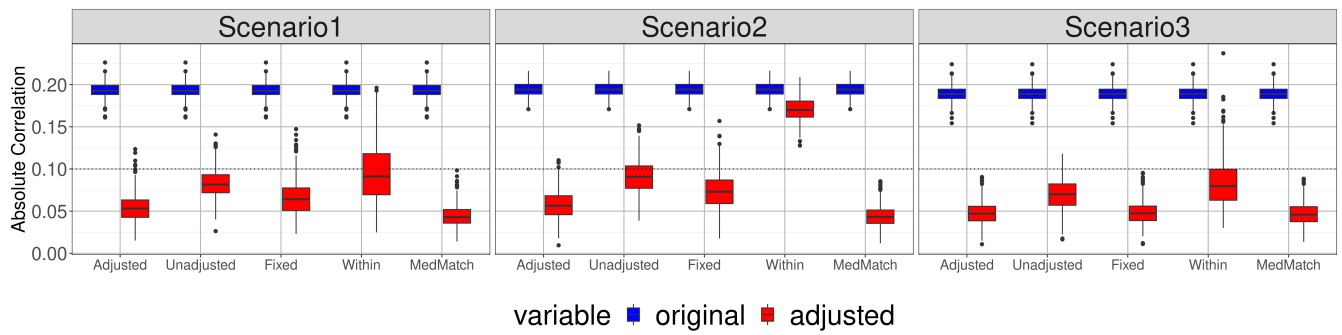


Figure S4: Simulation results: Average AC's (i.e. $\rho_{\{C,Z\}}$) in the original dataset (blue) and matched dataset (red) for each method (x-axis) and scenario (columns). Among 500 simulate datasets, the covariate balance is not met 40.8% for *within*, 6.2% for *fixed*, and 1.2% for *adjusted* in Scenario 1; 100% for *within*, 31.4% for *unadjusted*, 13.6% for *fixed*, and 1.6% for *adjusted* in Scenario 2; and 24.4% for *within*, and 4.8% for *unadjusted* in Scenario 3.

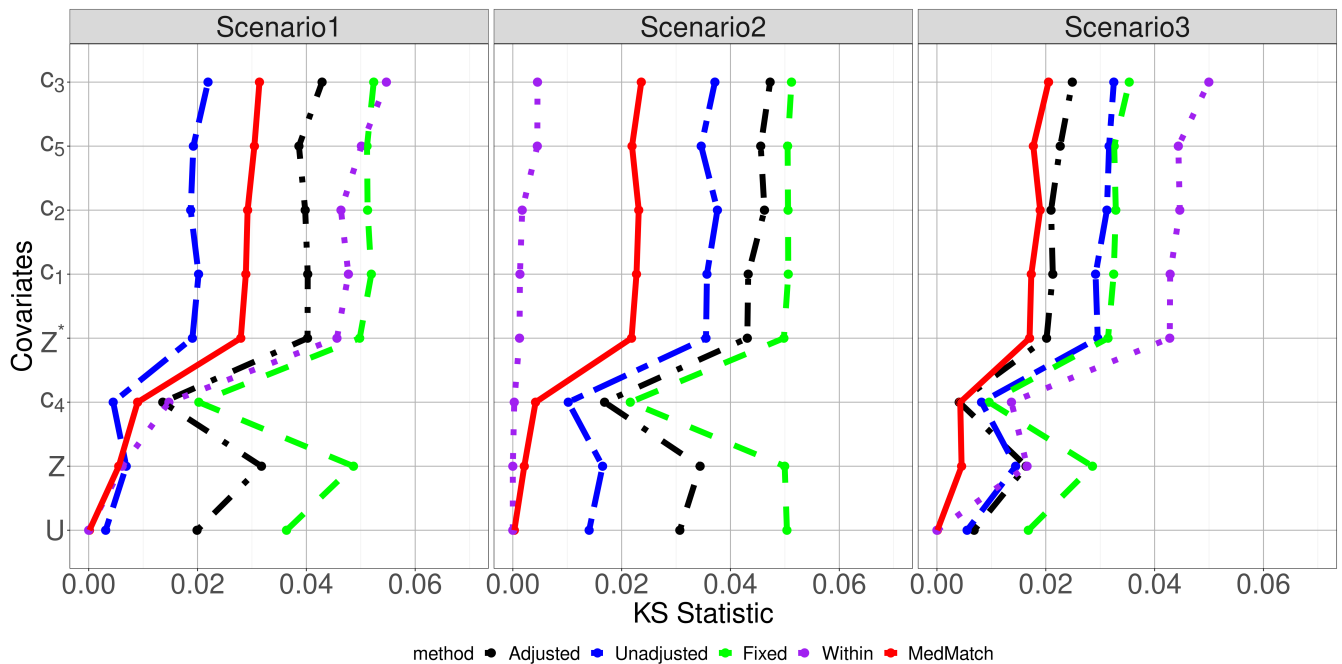


Figure S5: Simulation results: KS statistic for each covariate averaged across 500 simulated datasets for each method and scenario (columns). We assess whether matched data is well preserving the distribution of Z in the original data. The smaller the KS statistic, the higher the probability that the two distributions are the same. The *adjusted* is a black dot dashed line, *unadjusted* is a blue two dashed line, *fixed* is a green dashed line, *within* is a purple dotted line and *MedMatch* is a red solid line.

S.2 PM_{2.5} and Childhood Respiratory Outcomes in Medicaid

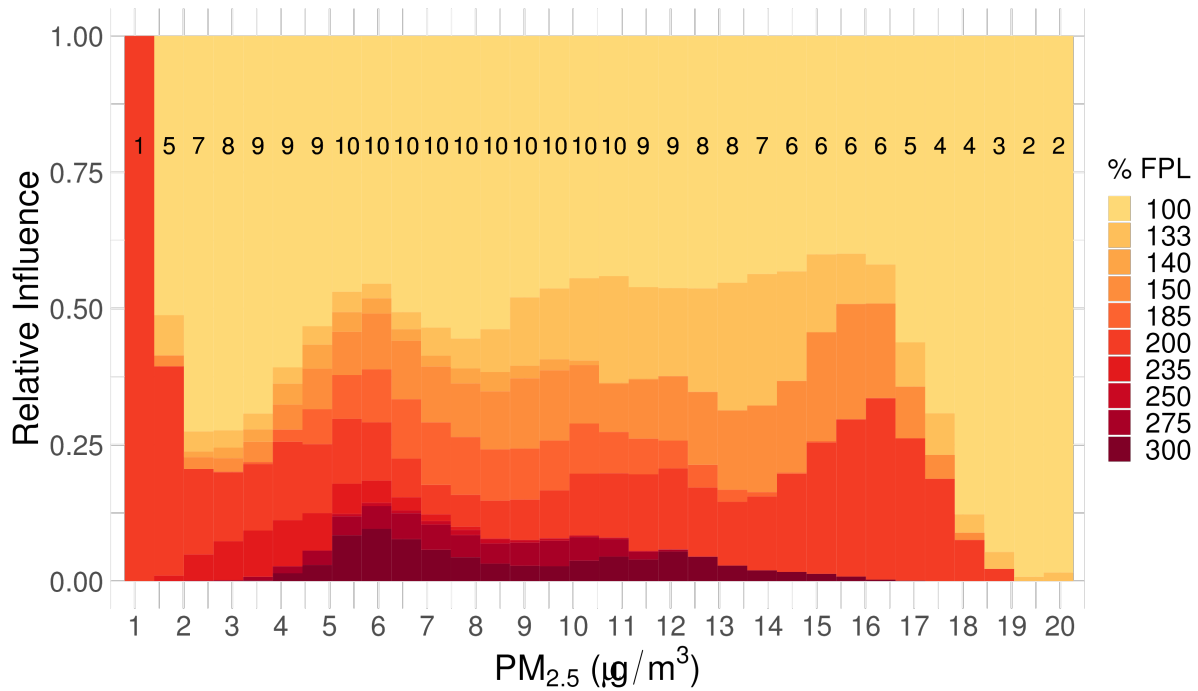


Figure S6: Relative contributions of each cluster on the at each exposure levels in the original data, color coded by Medicaid eligibility threshold (%FPL). The darker red indicates higher %FPL, i.e., a less stringent eligibility threshold. The black numbers at each exposure window represents the number of clusters that experienced exposure levels within that exposure window. Note that many clusters never experience extreme PM_{2.5} concentrations falling in the tails of the distribution (e.g. $PM_{2.5} \leq 2 \mu\text{g}/\text{m}^3$ or $PM_{2.5} \geq 18 \mu\text{g}/\text{m}^3$). To avoid violations of the positivity assumption, we only include units with observed exposures within the subset of the exposure range where at least 7 out of the 10 clusters are represented.

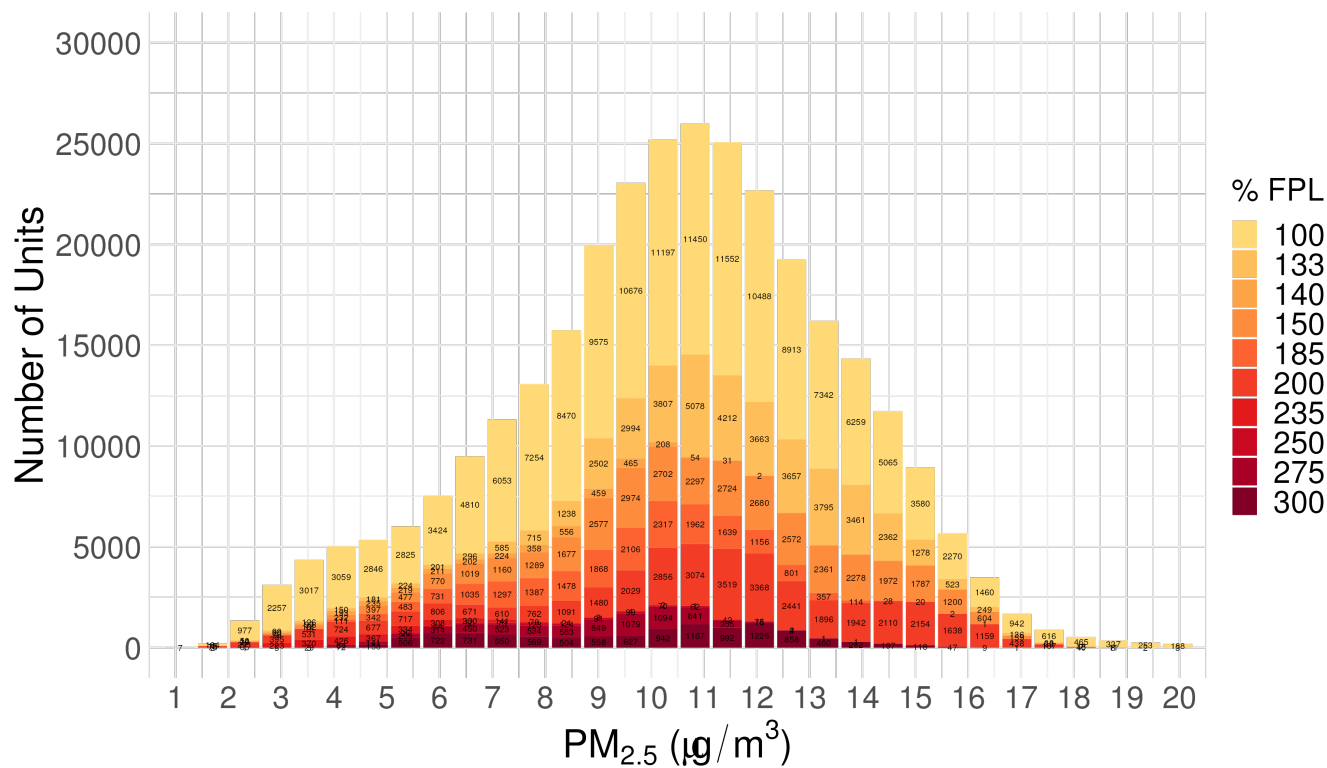


Figure S7: Number of units at each exposure levels in the original data during 2000-2012, color coded by Medicaid eligibility threshold (%FPL). The darker red indicates higher %FPL, i.e., a less stringent eligibility threshold. The number of units for each %FPL ranged from 825 to 148,933.

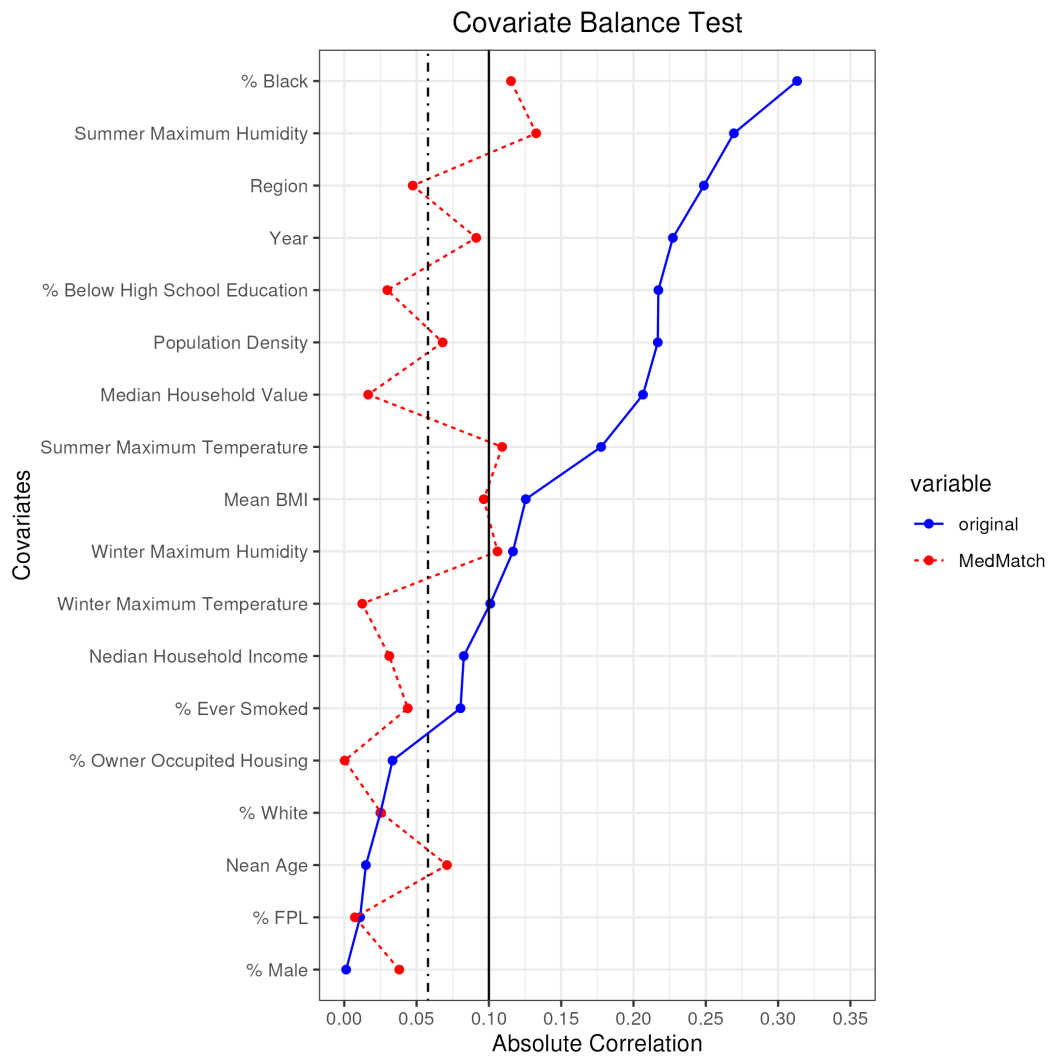


Figure S8: Absolute correlations for each covariate in the matched dataset (red dotted line) and original dataset (blue solid line) using *MedMatch*. The average AC improved from 0.14 prior to matching to 0.05 after matching, which is smaller than 0.1 cut-off of covariate balance (black dot dashed line).

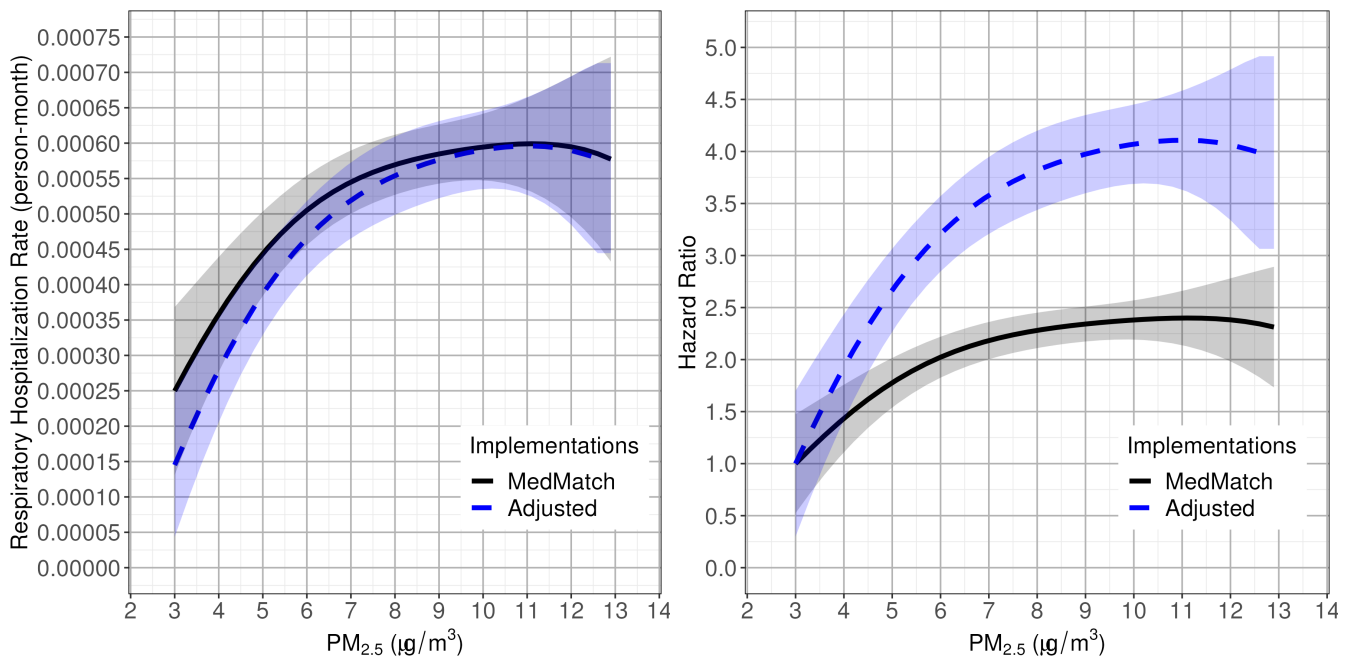


Figure S9: A comparison of causal ERFs relating respiratory hospitalization to long-term PM_{2.5} exposure in children enrolled in Medicaid (2000-2012) using *adjusted* and *MedMatch*. The black solid line represents estimated ERF estimated using *MedMatch* and blue dotted using *adjusted*. The shaded area represents corresponding pointwise Wald 95% confidence band. The optimal hyperparameter for *adjusted* was $(\delta, \lambda) = (0.30, 1)$ and mean AC was 0.06 with maximum of AC's equal to 0.12.

S.2.1 Data Description

We remove enrollees who provided a residential zip code that does not align with their state of Medicaid enrollment. Among the 48 contiguous US states, we exclude Kansas and Maine because Medicaid claims data for Maine from 2005-2010 and Kansas for 2010 are unavailable. Our unit of analysis is zip code-year and we remove zip code-years with less than 5 enrollees. As the eligibility limits were missing for years 2001 and 2007, we imputed with next year's eligibility limits.

To control for possible confounders, we adjust our analyses for sociodemographic, health behavior, and meteorological variables collated from various sources. First, from Medicaid enrollment records we collect the age, sex, and race of each enrollee in a given zip code and year and use these to construct zip code and year-specific mean age, proportion male, proportion white, and proportion Black for Medicaid beneficiaries. We also obtain county-level mean body mass index (BMI) and smoking rate from the CDC's Behavioral Risk Factor Surveillance System, and zip code level measures are constructed by assigning to each zip code the value of the measure in the county where the zip code's centroid lies. While smoking rate and BMI are not anticipated to be directly

interpretable as measures of health behaviors in children, we use them as proxies of general health consciousness in the local population. We extract the following six zip code level features from US Census data: median household income, median household value, proportion of housing units in each zip code occupied by their owner, population per square meter in each zip code, proportion of the population below the poverty line, proportion of the population not completing high school. We also adjust for four zip code level annual meteorological variables constructed from Google Earth Engine data - the summer (June to September) and winter (December to February) averages of maximum and minimum daily temperatures and relative humidity. In addition, we adjust all analyses for US region (Northeast, South, Midwest, and West) as a categorical variable and calendar year (2000-2012) (Wu et al., 2022, 2020).